ffeoylquinic_acids_and_flavonoids_in_Pluchea_indica_Less._le.pdf

by 1 1

Submission date: 07-Jan-2025 10:12AM (UTC+1000)
Submission ID: 2560439470
File name: ffeoylquinic_acids_and_flavonoids_in_Pluchea_indica_Less._le.pdf (1.83M)
Word count: 12138
Character count: 63800

© 2024 Journal of Pharmacy & Pharmacognosy Research, 12 (4), 701-721, 2024
ISSN 0719-4250
https://jppres.com

DOI: https://doi.org/10.56499/jppres23.1896_12.4.701

Original Article

A computational approach to evaluate caffeoylquinic acids and flavonoids in *Pluchea indica* Less. leaves as potential anti-HIV agents

[Un enfoque computacional para evaluar los ácidos cafeoilquínicos y los flavonoides de las hojas de *Pluchea indica* Less. como posibles agentes contra el VIH]

Ni Putu Ermi Hikmawanti[1,2,8], Fadlina Chany Saputri[3,8], Arry Yanuar[4,8], Ibrahim Jantan[5], Yeni Yeni[6], Abdul Mun'im[7,8*]

[1]Graduate Program of Pharmaceutical Sciences, Faculty of Pharmacy, Universitas Indonesia, Cluster of Health Sciences Building, Depok, 16424, West Java, Indonesia.
[2]Department of Pharmaceutical Biology, Faculty of Pharmacy and Sciences, Universitas Muhammadiyah Prof. DR. HAMKA, East Jakarta, 13460, DKI Jakarta, Indonesia.
[3]Department of Pharmacology-Toxicology, Faculty of Pharmacy, Universitas Indonesia, Depok, 16424, West Java, Indonesia.
[4]Department of Biomedical Computation-Drug Design, Faculty of Pharmacy, Universitas Indonesia, Depok, 16424, West Java, Indonesia.
[5]Institute of Systems Biology (INBIOSIS), Universiti Kebangsaan Malaysia, UKM Bangi, 43600, Selangor, Malaysia.
[6]Department of Pharmaceutical Chemistry, Faculty of Pharmacy and Sciences, Universitas Muhammadiyah Prof. DR. HAMKA, East Jakarta, 13460, DKI Jakarta, Indonesia.
[7]Department of Pharmacognosy-Phytochemistry, Faculty of Pharmacy, Universitas Indonesia, Cluster of Health Sciences Building, Depok, 16424, West Java, Indonesia.
[8]National Metabolomics Collaborative Research Center, Faculty of Pharmacy, Universitas Indonesia, Depok, West Java 16424, Indonesia.
*E-mail: munim@farmasi.ui.ac.id

Abstract

Context: The attachment of human immunodeficiency virus type 1 glycoprotein 120 (HIV-1 gp120) to the CD4 receptor of human immune cells is the beginning of HIV-1 infection. Stimulation of reactive oxygen species (ROS) production through upregulation of nicotinamide adenine dinucleotide phosphate (NADPH) oxidase-2 (NOX-2) and -4 (NOX-4), and cytochrome P450 2E1 (CYP2E1) of the virus can be a potential target for anti-HIV agents.

Aims: To evaluate the inhibitory effects of caffeoylquinic acids (CQAs) and flavonoids of *Pluchea indica* leaves against the binding of HIV-1 gp120 with CD4 receptor and their antioxidant activities via interactions with NOX-2, NOX-4, and CYP2E1 through *in silico* study.

Methods: Ten CQAs and nine flavonoids of *P. indica* were docked to the 3TGS (gp120 HIV-1), 2CDU (NOX-2), 3A1F (NOX-4), and 3T3Z (CYP2E1) receptors using the AutoDockTools 1.5.7. Physicochemical and pharmacokinetics properties were predicted using the pkCSM online tool, while toxicity was predicted using the ProTox-II webserver.

Results: Mostly, all of the CQAs and flavonoids were able to bind to all receptors. 3,4-Di-O-caffeoylquinic acid has the lowest binding energy (-8.79 kcal/mol) against 3TGS (gp120). 5-O-Caffeoylquinic acid and apigenin have great potential as antioxidants due to their good binding with NOX-2 and CYP2E1. However, CQAs might have ADME problems. Most test compounds did not cause hepatotoxicity, carcinogenicity, or mutagenicity. All test compounds have no cytotoxic potential. However, all CQAs have the potential to be immunotoxins.

Conclusions: The findings indicated that 3,4-di-O-caffeylquinic acid could be a potential inhibitor of HIV-1 gp120-CD4 binding, while 5-O-caffeoylquinic acid and apigenin demonstrated strong antioxidant activities via NOX-2 and CYP2E1 inhibition. However, in-depth studies, including experimental *in vitro* and *in vivo* studies, are required to validate the anti-HIV activity of the compounds further.

Keywords: antiviral; *in silico*; molecular docking; phenolics; *Pluchea indica*.

Resumen

Contexto: La unión de la glicoproteína 120 del virus de la inmunodeficiencia humana tipo 1 (VIH-1 gp120) al receptor CD4 de las células inmunitarias humanas es el inicio de la infección por VIH-1. La estimulación de la producción de especies reactivas de oxígeno (ROS) a través de la regulación al alza de la nicotinamida adenina dinucleótido fosfato (NADPH) oxidasa-2 (NOX-2) y -4 (NOX-4), y el citocromo P450 2E1 (CYP2E1) del virus puede ser un objetivo potencial para los agentes contra el VIH.

Objetivos: Evaluar los efectos inhibidores de los ácidos cafeoilquínicos (CQAs) y flavonoides de las hojas de *Pluchea indica* contra la unión de la gp120 del VIH-1 con el receptor CD4 y sus actividades antioxidantes vía interacciones con NOX-2, NOX-4, y CYP2E1 a través de un estudio *in silico*.

Métodos: Diez CQA y nueve flavonoides de *P. indica* se acoplaron a los receptores 3TGS (gp120 VIH-1), 2CDU (NOX-2), 3A1F (NOX-4) y 3T3Z (CYP2E1) utilizando AutoDockTools 1.5.7. Las propiedades fisicoquímicas y farmacocinéticas se predijeron con la herramienta en línea pkCSM. Las propiedades fisicoquímicas y farmacocinéticas se predijeron con la herramienta en línea pkCSM, mientras que la toxicidad se predijo con el servidor web ProTox-II.

Resultados: En general, todos los CQAs y flavonoides fueron capaces de unirse a todos los receptores. El ácido 3,4-Di-O-cafeilquínico tiene la energía de unión más baja (-8,79 kcal/mol) frente a 3TGS (gp120). El ácido 5-O-cafeilquínico y la apigenina tienen un gran potencial como antioxidantes debido a su buena unión con NOX-2 y CYP2E1. Sin embargo, los ACQ podrían tener problemas de ADME. La mayoría de los compuestos de prueba no causaron hepatotoxicidad, carcinogenicidad ni mutagenicidad. Todos los compuestos de ensayo no tienen potencial citotóxico. Sin embargo, todos los CQAs tienen el potencial de ser inmunotoxinas.

Conclusiones: Los resultados indicaron que el ácido 3,4-di-O-cafeilquínico podría ser un inhibidor potencial de la unión gp120-CD4 del VIH-1, mientras que el ácido 5-O-cafeilquínico y la apigenina demostraron fuertes actividades antioxidantes a través de la inhibición de NOX-2 y CYP2E1. Sin embargo, se requieren estudios en profundidad, incluyendo estudios experimentales *in vitro* e *in vivo*, para validar aún más la actividad anti-VIH de los compuestos.

Palabras Clave: acoplamiento molecular; antiviral; fenoles; *in silico*; *Pluchea indica*.

ARTICLE INFO
Received: November 22, 2023.
Accepted: March 14, 2024.
Available Online: March 24, 2024.

AUTHOR INFO
ORCID: 0000-0001-5194-1431 (NPEH) 0000-0001-9066-4780 (IJ)
0000-0002-6668-8915 (FCS) 0000-0001-9042-4824 (YY)
0000-0001-8895-9010 (AY) 0000-0002-6681-9196 (AM)

Abbreviations: ADME: Absorption, distribution, metabolism, and excretion; AIDS: Acquired immunodeficiency syndrome; ARV: Antiretroviral; BBB: Blood-brain barrier; CNS: Central nervous system; CQAs: Caffeoylquinic acids; CYP: Cytochrome P450; GHS: Globally Harmonized System of Classification and Labelling; Gp120: Glycoprotein 120; Gp41: Glycoprotein 41; HIV-1: Human immunodeficiency virus type 1; Ki: Inhibition constant; LD_{50}: Lethal dosage 50; NADPH: Nicotinamide adenine dinucleotide phosphate; NOX: NADPH oxidase; OCT2: Organic cation transport 2; POX: Proline oxidase; RMSD: Root mean square deviation: ROS: Reactive oxygen species; VDss: Volume distribution.

INTRODUCTION

Human immunodeficiency virus type 1 (HIV-1) is a lentivirus that infects the human immune system (World Health Organisation, 2023), especially cells with CD4 receptors on their surface, such as T helper cells, macrophages, dendritic cells, and astrocytes (Seitz, 2016). In 2022, 39 million people were living with HIV in the world (World Health Organisation, 2023). Until now, treatment with antiretroviral (ARV) is still the primary choice for suppressing viral replication (Shin et al., 2021). Targets for HIV replication inhibition from ARV include attachment, fusion or entry, and viral enzymes (Popović-Djordjević et al., 2022; Sierra-Aragón and Walter, 2012).

Attachment is an early stage in the HIV-1 life cycle, which can be a crucial target with great opportunities in the discovery and development of ARV (Caffrey, 2011), HIV-1 pre-exposure prophylaxis therapy (Malik et al., 2017; Mirani et al., 2019), even protection from infection (Bruxelle et al., 2021). Glycoprotein 120 (gp120) is one of the HIV-1 proteins (besides gp41) that plays a role in the initial attachment (Malik et al., 2017). Gp120 has also been reported to play a role in stimulating the production of reactive oxygen species (ROS), such as $O_2^{\bullet-}$ and H_2O_2, in various cell lines (i.e., astrocytes and microglia) (Ivanov et al., 2016; Reshi et al., 2014). Stimulation of ROS production occurs through upregulation of cytochrome P450 2E1 (CYP2E1), proline oxidase (POX), and activation of the nicotinamide adenine dinucleotide phosphate (NADPH) oxidase-2 (NOX-2) and -4 (NOX-4) (Ivanov et al., 2016). High amounts of ROS can increase the risk of accelerating the progression of infection towards acquired immunodeficiency syndrome (AIDS) (Reshi et al., 2014). Fostemsavir is a first-in-class drug as an attachment inhibitor, which was approved by the United States (US) Food Drugs Association (FDA) in July 2020 for the treatment of patients with multi-drug-resistant HIV-1 infection (Hiryak and Koren, 2021). However, as with other ARVs, the possibility of adverse side effects (viz., poor tolerability, toxicities, and drug-drug interactions, among others), availability of types and affordability of drugs in certain countries (Forsythe et al., 2019) are challenges. Thus, the discovery and development of new medicinal compounds are urgently needed.

Several natural compounds have been reported as sources of medicinal chemicals with anti-HIV properties (Najmi et al., 2022; Popović-Djordjević et al., 2022; Salehi et al., 2018), such as polyphenolics (including phenolics, flavonoids, lignans, tannins), coumarins, and alkaloids, which target the HIV-1 life cycle (Kaur et al., 2020; Popović-Djordjević et al., 2022). *Asteraceae* is a family of herbs that is rich in phenolic hydroxycinnamic acid derivatives (one of which is caffeoylquinic acids, CQAs) and flavonoids, which are beneficial for protecting human health (Rolnik and Olas, 2021). Both classes of natural compounds have been shown to have anti-HIV activity against reverse transcriptase (Mahmood et al., 1993; Phosrithong et al., 2012; Tamayose et al., 2019b), integrase (Hu et al., 2010; McDougall et al., 1998; Serina et al., 2016), and protease (McDougall et al., 1998; Serina et al., 2016). They also have good antioxidant activity (Heim et al., 2002; Lu et al., 2020; Magaña et al., 2021; Marković and Tošović, 2016; Tamayose et al., 2019a). *Pluchea indica* Less. is one of many members of the *Asteraceae,* whose leaves have been identified to contain several types of CQAs and flavonoids. CQAs are the major active compounds in *P. indica* leaves (Kongkiatpaiboon et al., 2018). Traditionally, the leaves are used to treat digestive diseases caused by bacteria or parasitic infections (Hikmawanti et al., 2024). Decoction of the leaves in boiling water is used to treat tuberculosis symptoms (Alvin et al., 2014). The antiviral potential of *P. indica* leaves has also been reported against HIV-1 (Locher et al., 1996; Wardani et al., 2018) and hepatitis B virus (HBV) (Indrasetiawan et al., 2019). Thus, studying the CQAs and flavonoid components of *P. indica* leaves as potential HIV-1 attachment inhibitors is interesting.

Generally, drug discovery and development from medicinal plants begin with metabolite extraction, purification, preclinical testing, and clinical trials on humans. The different stages can take a long time, require a lot of energy, and be very costly. In addition, the failure rate at the clinical trial stage is very high, with possibly only one out of 5000 lead compounds reaching the market for therapeutic use (Ezzat et al., 2019). Recently, computational approaches have been used to screen candidate compounds to be developed as drugs particularly through *in silico* molecular docking studies (Najmi et al., 2022; Shaker et al., 2021). Through molecular docking studies, predictions of interactions and binding affinity between candidate compounds and target receptors can be studied simultaneously. In addition, the assessment

of pharmacokinetic properties, such as ADME and toxicity, can be done *in silico* (Rudrapal and Chetia, 2020).

Therefore, the evaluation of CQAs and flavonoids from *P. indica* leaves as anti-HIV targeting gp120 HIV-1 and antioxidants targeting interactions with CYP2E1, NOX-2, and NOX-4 through computational molecular docking studies was carried out. Their performance was also compared with reference drugs, such as fostemsavir, BMS-806, dextromethorphan, apocynin, and propofol. In addition, *in silico* ADME and toxicity of the tested CQAs and flavonoids were also predicted in this study.

MATERIAL AND METHODS

Instrumentation

The research was conducted using Windows 11 Home Single Language 64-bit (10.0, Build 22621). The processor used was AMD RYZEN 5 4500U with Radeon Graphics (6CPUs, ~2.4 GHz) and memory 8192MB RAM.

Molecular docking

Preparation of proteins

The type of target receptors, their characteristics, and the positive controls used in this study are presented in Table S1. Before docking, each receptor was prepared by removing water molecules and ions from the receptor molecule. The native ligand was separated from the receptor molecule. Polar hydrogen was added to the receptor structure. Receptor structure preparation was carried out with PyMol (v.2.5.5). Fig. S1 shows the structures of the receptors that were prepared and used in this study.

Preparation of ligands

The ligands used in this study were compounds from the CQA and flavonoid groups found in *P. indica* leaves through literature searches. The list of ligands used in this study is presented in Table 1. The structure of each compound was downloaded from the PubChem database (https://pubchem.ncbi.nlm.nih.gov/). Optimization of the shape of 3D compounds was carried out by adding hydrogen and minimizing energy using Avogadro2. Once completed, the file was saved in the pdb format.

Validation of the docking method

The docking method was validated by re-docking the native ligand on the active site of the receptor. The docking method validation parameters were met if the root mean square deviation (RMSD) value was <2 Å. Specifically for the 3A1F receptor, the docking method was validated using VAS2870 on the binding pocket previously predicted by Vinay et al. (2020).

Docking assay

Initially, the receptor and ligand file format in pdb was changed to pdbqt. Central grid points for each receptor used in this study, viz., -20.864(x), -3.978(y), 19.876(z) for 3TGS; 15.597(x), -13.324(y), 10.201(z) for 3A1F; 18.427(x), -6.355(y), -1.793(z) for 2CDU; and 24.468(x), 26.146(y), 13.305(z) for 3T3Z, respectively. The dimensions of the grid box used were 44 × 44 × 44 for 3TGS, 66 × 56 × 54 for 3A1F, 30 × 24 × 32 for 2CDU, and 40 × 40 × 40 for 3T3Z. Spacing was specified on 0.375 Å. The grid box settings were saved in gpf format and then ran AutoGrid. The docking process in this study used the following genetic algorithm parameter settings: number of GA runs = 100, Population size = 150, maximum number of evals = medium (2 500 000), and other parameters were in default conditions. The Lamarckian GA (4.2) output was saved in dpf format and then run by AutoDockTools 1.5.7. The docking results in the form of files in dlg format were analyzed using Notepad ++ (v8.5.4) software. Visualization of docking results was carried out using Discovery Studio Visualizer 2021 (v21.1.0.20298).

Table 1. Compounds used in this study.

Compound	Synonym*	Code	PubChem CID*	Molecular formula*	Chemical structure**	Ref.
Caffeoylquinic acids (CA):						
3-O-Caffeoylquinic acid	Chlorogenic acid	CA1	1794427	$C_{16}H_{18}O_9$	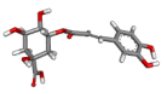	Phewchida and Vongsak, 2019; Kongkiatpaiboon et al., 2018; Vongsak et al., 2018)

Table 1. Compounds used in this study(continued.)..

Compound	Synonym*	Code	PubChem CID*	Molecular formula*	Chemical structure**	Ref.
4-O-Caffeoylquinic acid	Crypto chlorogenic acid	CA2	9798666	$C_{16}H_{18}O_9$	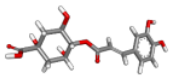	(Chewchida and Vongsak, 2019; Kongkiatpaiboon et al., 2018; Vongsak et al., 2018)
5-O-Caffeoylquinic acid	Neochlorogenic acid	CA3	5280633	$C_{16}H_{18}O_9$	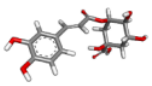	(Chewchida and Vongsak, 2019; Kongkiatpaiboon et al., 2018; Vongsak et al., 2018)
3,4-Di-O-Caffeoylquinic acid	Iso chlorogenic acid B	CA4	5281780	$C_{25}H_{24}O_{12}$	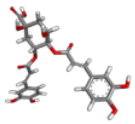	(Chewchida and Vongsak, 2019; Kongkiatpaiboon et al., 2018; Vongsak et al., 2018)
3,5-Di-O-Caffeoylquinic acid	Iso chlorogenic acid A	CA5	6474310	$C_{25}H_{24}O_{12}$	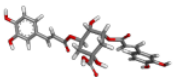	(Chewchida and Vongsak, 2019; Kongkiatpaiboon et al., 2018; Vongsak et al., 2018)
4,5-Di-O-Caffeoylquinic acid	Iso chlorogenic acid C	CA6	6474309	$C_{25}H_{24}O_{12}$	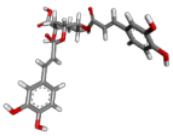	(Chewchida and Vongsak, 2019; Kongkiatpaiboon et al., 2018; Vongsak et al., 2018)
4,5-Di-O-Caffeoylquinic acid methyl ester	-	CA7	10052718	$C_{26}H_{26}O_{12}$	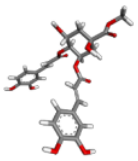	(Arsiningtyas et al., 2014)
3,4,5-Tri-O-Caffeoylquinic acid	-	CA8	6440783	$C_{34}H_{30}O_{15}$	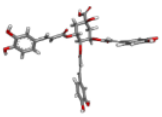	(Arsiningtyas et al., 2014)
3,4,5-Tri-O-Caffeoylquinic acid methyl ester	-	CA9	53239460	$C_{35}H_{32}O_{15}$	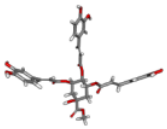	(Arsiningtyas et al., 2014)
1,3,4,5-Tetra-O-Caffeoylquinic acid	-	CA10	5281799	$C_{43}H_{36}O_{18}$	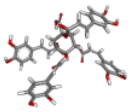	(Arsiningtyas et al., 2014)

Table 1. Compounds used in this study(continued…)

Compound	Synonym*	Code	PubChem CID*	Molecular formula*	Chemical structure**	Ref.
Flavonoids (F):						
Quercetin	-	F1	5280343	$C_{15}H_{10}O_7$	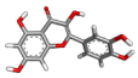	(Andarwulan et al., 2010)
Kaempferol	-	F2	5280863	$C_{15}H_{10}O_6$	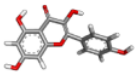	(Andarwulan et al., 2010)
Myricetin	-	F3	5281672	$C_{15}H_{10}O_8$	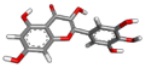	(Andarwulan et al., 2010)
Luteolin	-	F4	5280445	$C_{15}H_{10}O_6$	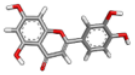	(Andarwulan et al., 2010)
Apigenin	-	F5	5280443	$C_{15}H_{10}O_5$	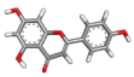	(Andarwulan et al., 2010)
Quercetin 3-O-rhamnoside	Quercitrin	F6	5280459	$C_{21}H_{20}O_{11}$	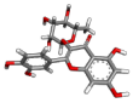	(Hussin et al., 2019)
Quercetin 3-O-glucoside	Isoquercetin	F7	5280804	$C_{21}H_{20}O_{12}$	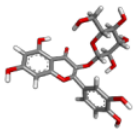	(Hussin et al., 2019)
Quercetin 3-O-glucuronide	Miquelianin	F8	5274585	$C_{21}H_{18}O_{13}$	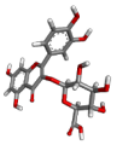	(Hussin et al., 2019)
Kaempferol 3-O-β-D-glucopyranoside	Astragalin	F9	5282102	$C_{21}H_{20}O_{11}$	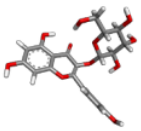	(Hussin et al., 2019)

Table 1. Compounds used in this study(continued...)

Compound	Synonym*	Code	PubChem CID*	Molecular formula*	Chemical structure**	Ref.
Reference drugs (RD):						
Fostemsavir	BMS-663068 free acid	RD1	11319217	$C_{25}H_{26}N_7O_8P$	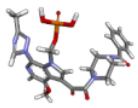	(Lai, 2021)
BMS-806	BMS-378806	RD2	5495818	$C_{22}H_{22}N_4O_4$	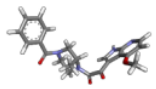	(Tintori et al., 2013)
Dextromethorphan	d-Methorphan	RD3	5360696	$C_{18}H_{25}NO$	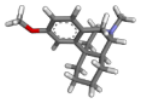	(Da Silva Costa et al., 2018)
Propofol	2,6-diisopropylphenol	RD4	4943	$C_{12}H_{18}O$	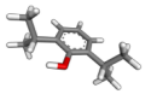	(Lewis et al., 2000)
Apocynin	Apocynin A	RD5	9804654	$C_{24}H_{20}O_{10}$	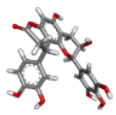	(Mhya et al., 2023)

*From PubChem database (https://pubchem.ncbi.nlm.nih.gov/); **Visualization from Discovery Studio 2021.

Determination of predicted physicochemical parameters

Prediction of these parameters was carried out via the pkCSM webserver (https://biosig.lab.uq.edu.au/pkcsm/prediction), which was accessed for free. The respective ligand molecules were uploaded in canonical SMILE format. The parameters of the physicochemical properties of each ligand determined in this study were molecular weight (g/mol), log P, number of rotatable bonds, hydrogen bond donors, hydrogen bond acceptors, and surface area.

Determination of ADME parameter predictions

ADME parameter predictions were carried out to obtain an overview of the properties of adsorption (A), distribution (D), metabolism (M), and excretion (E). The adsorption parameters determined include water solubility (A_1), Caco-2 permeability (A_2), intestinal absorption (human) (A_3), skin permeability (A_4), P-glycoprotein substrate (A_5), P-glycoprotein I inhibitor (A_6), and P-glycoprotein II inhibitor (A_7). The distribution parameters determined include volume distribution (VDss), human) (D_1), fraction unbound (human) (D_2), blood-brain barrier (BBB) permeability (D_3), and central nervous system (CNS) permeability (D_4). The metabolic parameters determined include CYP2D6 substrate (M_1), CYP3A4 substrate (M_2), CYP1A2 inhibitor (M_3), CYP2C19 inhibitor (M_4), CYP2C9 inhibitor (M_5), CYP2D6 inhibitor (M_6), and CYP3A4 inhibitor (M_7). The specified excretion parameters were total clearance (E_1) and renal organic cation transport 2 (OCT_2) substrate (E_2).

Determination of predicted toxicity parameters

Prediction of toxicity parameters for each ligand was carried out using the ProTox-II, which was accessed for free via https://tox-new.charite.de/protox_II/). The predicted toxicity parameters were the lethal dosage 50 (LD_{50}) value, toxicity class, hepatotoxicity, carcinogenicity, immunotoxicity, mutagenicity, and cytotoxicity properties of each compound.

Data analysis

Validation of the docking method was accepted if the RMSD value of the redocking result was <2 Å. The binding affinity energy (ΔG) and the inhibition constant (Ki) values from the molecular docking study of each CQA and flavonoid tested were compared with

each reference drug. In addition, chemical interactions between residues on the target protein and the tested ligand with the most negative binding affinity energy values were observed and presented in the form of 2D images using Discovery Studio Visualizer 2021 (v21.1.0.20298). Predictions of the physicochemical properties of each compound investigated were compared with the Lipinski rule (Turner and Agatonovic-Kustrin, 2007). The ADME and toxicity predictions for each compound tested were compared with the criteria for each test parameter based on literature (if any).

RESULTS

Evaluation of molecular docking

The overlay of the native ligand crystal with the re-docked ligand is presented in Fig. 1. Based on the results obtained, the RMSD value of each re-docked native ligand gave a result of <2.0 Å. It means that the docking method can be used to dock the compounds being tested. Meanwhile, blind-docking was carried out on the 3A1F receptor using ordinates and grid box dimensions based on a study by Vinay et al. (2020).

The docking results of the CQAs and flavonoids of *P. indica* leaves are presented in Table 2. From the CQAs group, the lowest binding energy value compared to other CQAs against the 3TGS (gp120 HIV-1) receptor was 3,4-di-O-caffeoylquinic acid (–8.79 kcal/mol), against the 3A1F (NOX-4) receptor was 4-O-caffeoylquinic acid (–5.56 kcal/mol), against the 2CDU (NOX-2) receptor is the 5-O-caffeoylquinic acid (–7.98 kcal/mol), and against the 3T3Z (CYP2E1) was 5-O-caffeoylquinic acid (–6.18 kcal/mol). From the flavonoids group, the lowest binding energy compared to other flavonoids against the 3TGS (gp120 HIV-1) receptor was quercetin 3-O-glucoside (–7.38 kcal/mol), against the 3A1F (NOX-4) receptor was quercetin 3-O-glucuronide (–5.73 kcal/mol), against the 2CDU (NOX-2) receptor was the apigenin (–7.33 kcal/mol), and against the 3T3Z (CYP2E1) was apigenin (–8.91 kcal/mol).

Figure 2 shows the 2D interaction between the ligands with the lowest binding energy and residues around the binding pocket of the 3TGS receptor. Ligand 03G, as a native ligand of 3TGS, interacted with Glu429, Met426, Gly473, and Asn425 residues via hydrogen bonds. In addition, ligand 03G also interacted with Phe382 and Val255 residues via Pi-alkyl and Phe376 residues via halogen Cl interactions. 3,4-Di-O-Caffeoylquinic acid interacted with Asn425, Gly431, Asp368, and Gln428 residues via hydrogen bonds, Val255 residue via Pi-alkyl interactions, and Trp427 residue via Pi-lone pair interactions. Quercetin 3-O-glucoside interacted with Asn425, Glu370, Asp368, Asp474, Met426, Gly431, and Gln428 residues via hydrogen bonds and Val430 residue via Pi-Sigma interactions. Fostemsavir interacted with Trp427 residue via hydrogen bonds, Val430 residue via Pi-alkyl, Ile424 residue via Pi-Sigma, and Glu429 residue via stacked amide-Pi interactions. Meanwhile, BMS-806 interacted with Glu429 and Met427 residues via hydrogen bonds and Val430 residues via Pi-alkyl interactions.

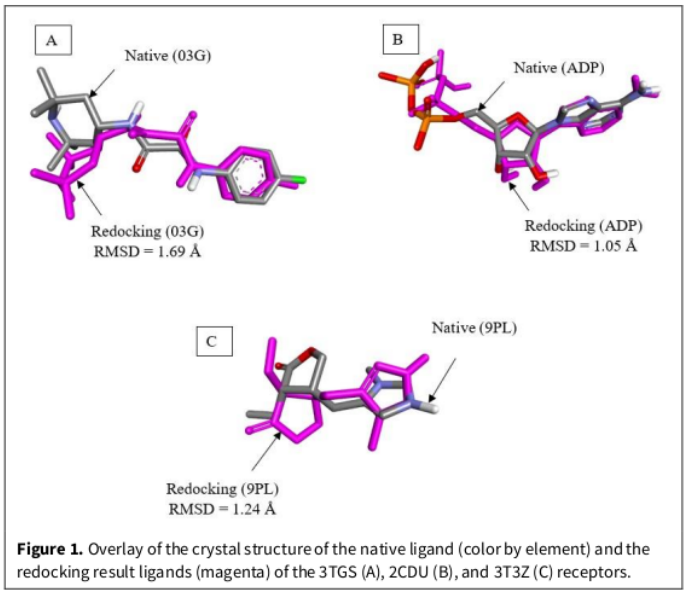

Figure 1. Overlay of the crystal structure of the native ligand (color by element) and the redocking result ligands (magenta) of the 3TGS (A), 2CDU (B), and 3T3Z (C) receptors.

Table 2. Molecular docking results of selected *P. indica* compounds.

Compound Codes	3TGS (gp120 HIV-1)		3A1F (NOX-4)		2CDU (NOX-2)		3T3Z (CYP2E1)	
	ΔG (kcal/mol)	Ki (μM)	ΔG (kcal/mol)	Ki (μM)	ΔG (kcal/mol)	Ki (μM)	ΔG (kcal/mol)	Ki (μM)
03G*	−10.39	0.02	nd	nd	nd	nd	nd	nd
VAS2870	nd	nd	−6.21	27.88	nd	nd	nd	nd
ADP*	nd	nd	nd	nd	−9.08	0.22	nd	nd
9PL*	nd	nd	nd	nd	nd	nd	−6.61	14.39
CA1	−6.82	10.00	−5.03	205.97	−6.91	8.65	−5.85	51.87
CA2	−6.27	25.35	−5.56	83.36	−6.74	11.56	−4.93	245.07
CA3	−6.59	14.84	−5.21	151.44	−7.98	1.41	−6.18	29.73
CA4	−8.79	0.36	−5.43	103.83	−7.41	3.70	−0.37	5.37×10^5
CA5	−8.58	0.52	−4.69	364.56	−4.85	277.22	−5.10	183.38
CA6	−7.30	4.45	−4.93	241.95	−6.58	14.92	-	-
CA7	−8.52	0.57	−4.72	344.87	−6.53	16.44	-	-
CA8	−6.59	14.83	−3.38	3.31×10^3	-	-	-	-
CA9	−6.92	8.42	−3.96	1.26×10^3	−0.27	6.37×10^5	-	-
CA10	−5.76	60.32	−2.90	7.50×10^3	-	-	-	-
F1	−6.82	10.05	−5.26	140.43	−6.96	7.97	−6.64	13.60
F2	−6.59	14.65	−4.79	307.92	−6.51	16.80	−6.34	22.35
F3	−6.83	9.93	−4.88	265.71	−6.90	8.81	−5.54	86.42
F4	−6.90	8.82	−5.03	205.58	−6.84	9.64	−7.60	2.68
F5	−7.27	4.68	−5.26	139.67	−7.33	4.21	−8.91	0.29
F6	−7.37	3.96	−5.37	115.04	−5.87	49.85	−3.57	2.43×10^3
F7	−7.38	3.87	−5.29	133.13	−5.42	105.72	−1.08	1.61×10^5
F8	−6.57	15.27	−5.73	63.37	−5.08	189.49	-	-
F9	−7.07	6.62	−5.54	87.33	−5.66	70.49	−2.81	8.73×10^3
RD1	−8.01	1.34	nd	nd	nd	nd	nd	nd
RD2	−8.28	0.86	nd	nd	nd	nd	nd	nd
RD3	nd	nd	−5.15	166.59	−6.83	9.84	nd	nd
RD4	nd	nd	nd	nd	nd	nd	−6.41	20.17
RD5	nd	nd	−5.91	46.82	−4.66	386.76	nd	nd

*Native ligand, CA1: 3-O-Caffeoylquinic acid, CA2: 4-O-Caffeoylquinic acid, CA3: 5-O-Caffeoylquinic acid, CA4: 3,4-Di-O-Caffeoylquinic acid, CA5: 3,5-Di-O-Caffeoylquinic acid, CA6: 4,5-Di-O-Caffeoylquinic acid, CA7: 4,5-Di-O-Caffeoylquinic acid methyl ester, CA8: 3,4,5-Tri-O-Caffeoylquinic acid, CA9: 3,4,5-Tri-O-Caffeoylquinic acid methyl ester, CA10: 1,3,4,5-Tetra-O-Caffeoylquinic acid, F1: Quercetin, F2: Kaempferol, F3: Myricetin, F4: Luteolin, F5: Apigenin, F6: Quercetin 3-O-rhamnoside, F7: Quercetin 3-O-glucoside, F8: Quercetin 3-O-glucuronide, F9: Kaempferol 3-O-β-D-glucopyranoside, RD1: Fostemsavir, RD2: BMS-806, RD3: Dextromethorphan, RD4: Propofol, RD5: Apocynin, nd: not determined, (-): poor binding energy (positive value), ΔG: free energy of binding, Ki: Inhibition constant, μM: micromolar.

Fig 3 presents the 2D interaction between the ligand with the lowest binding energy and residues around the binding pocket of the 3A1F receptor. VAS2870 was the ligand used to validate the docking method for this receptor, according to that carried out by Vinay et al. (2020). VAS2870 interacted with Ile139 residue via Pi-Alkyl, Glu135, and Lys54 residues via Pi-Cation/Pi-Anion, and Asn93, Ser91, Tyr56, Gln142, and Tyr58 residues via Pi-donor hydrogen bonds. 4-O-Caffeoylquinic acid interacted with Gln123, Asn93, Tyr95, Ser91, and Gln142 residues via hydrogen bonds and Glu135 residue via Pi-Anion. Quercetin 3-O-glucuronide interacted with Ser91, Gln142, Gln123, and Glu135 residues via hydrogen bonds and Thr138 via Pi-Sgma. Dextromethorphan interacted with Ser91 residue via a hydrogen bond, Ile139 residue via a Pi-

Alkyl bond, and Tyr56 and Gln142 residues via a carbon-hydrogen bond. Apocynin interacts with Lys124, Ser91, Gln123, and Glu135 residues via hydrogen bonds and Leu126 residue via Pi-Alkyl.

Fig. 4 shows the 2D interactions between ligands with low binding energy and residues around the binding pocket of the 2CDU receptor. The ADP native ligand interacted with Cys242, Gly161, Tyr188, Tyr159, Ile160, Gly244, His181, Asp179, Gly180, and Val 214 residues via hydrogen bond interactions, Gly156 residue via carbon-hydrogen bond, Lys213 residue via Pi-alkyl, and Ile243 residue via Pi-Sigma. 5-O-Caffeoylquinic acid interacted with Gly161, Cys242, Lys187, Asp179, and Lys213 residues via hydrogen bonds and His181 residue via carbon-hydrogen bonds. Apigenin interacted with Lys187, Val214, and Cys242 residues via a hydrogen bond, Lys213 residue via Pi-Alkyl, His181 residue via a carbon bond, and Asp179 residue via Pi-Anion. Dextromethorphan interacted with Arg183 and Asp179 residues via carbon-hydrogen bond, Ile243, and His181 residues via Pi-Alkyl, Lys187 residue via Pi-Cation, and Ser157 residue via Amide-Pi Stacked. Apocynin interacted with Cys242, His181, Asp179, and Ile243 residue via hydrogen bond, Gly180 residue via van der Waals, and Lys213 and Lys187 residues via Pi-Cation.

2D interactions of ligands with low binding energy to residues around the 3T3Z receptor binding pocket are shown in Fig. 5. 9PL (pilocarpine), as a native ligand of 3T3Z, interacted with Thr303 residue via hydrogen bonds, Phe207 residue via Pi-Alkyl bond, and HEM500 via Pi-Sigma bond. 5-O-caffeoylquinic acid interacted with Ala299 and Thr303 residues via hydrogen bonds, Leu103, Leu210 and Leu368 residues via Pi-Alkyl bond, and Phe116 residue via Pi-Pi T-shape bond. Apigenin interacted with Ala299 and Thr303 residues via hydrogen bonds, Leu210, Leu 115, and Leu368 residues via the Pi-Alkyl bond, Phe298, and Phe116 residues via Pi-Pi T-shaped bond, and Hem500 residue via unfavourable bump. The propofol interacted with Hem500 and Thr303 residues via the Pi-Sigma bond and Ala299 residue via the Pi-Alkyl bond.

The tested compounds are predicted to provide low binding affinity energy (Δ22 and show the best inhibition constant (Ki) value. For example, 3,4-di-O-caffeoylquinic acid has a Ki value of 0.36 μM (for 3TGS, gp120 HIV-1) lower than the Ki value of the reference drugs (Fostemsavir, Ki = 1.34 μM and BMS-806, Ki = 0.86 μM) for 3TGS. Otherwise, if the binding affinity energy is high, then the Ki value of the test compound is poor.

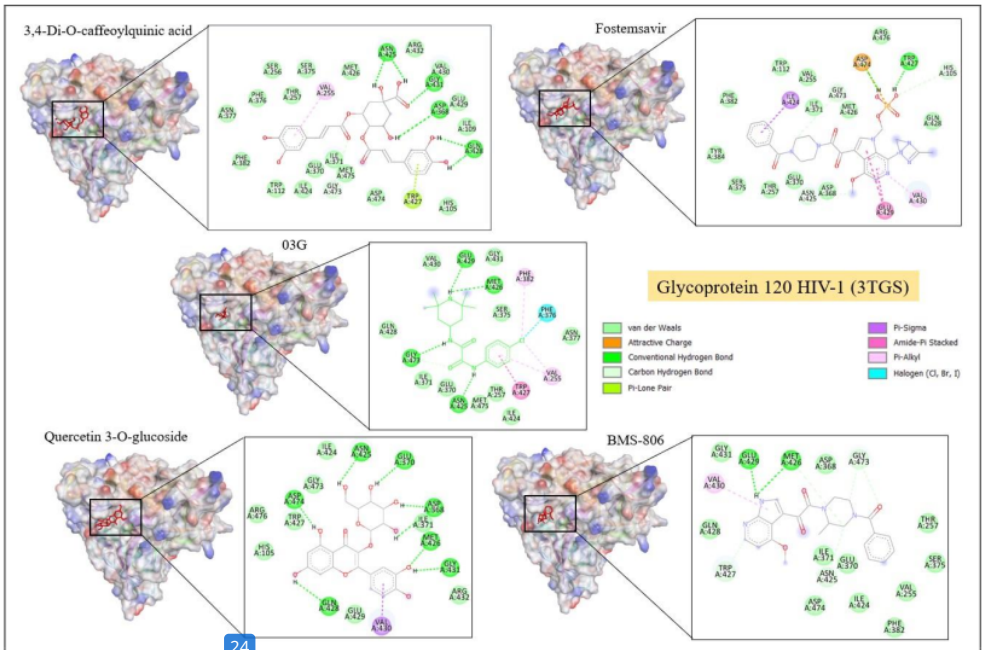

Figure 2. Interaction of 03G, 3,4-Di-O-caffeoylquinic acid, quercetin 3-O-glucoside, fostemsavir, and BMS-806 with residues in the binding pocket of the 3TGS receptor.

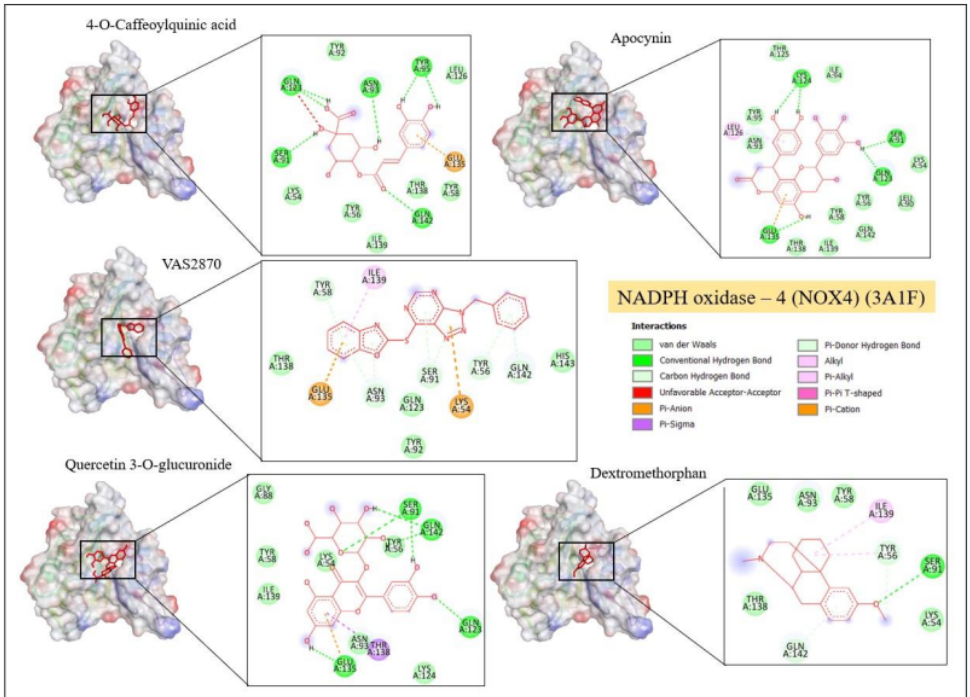

Figure 3. Interaction of VAS2870, 4-O-caffeoylquinic acid, quercetin 3-O-glucuronide, apocynin, and dextromethorphan with residues in the binding pocket of the 3A1F receptor.

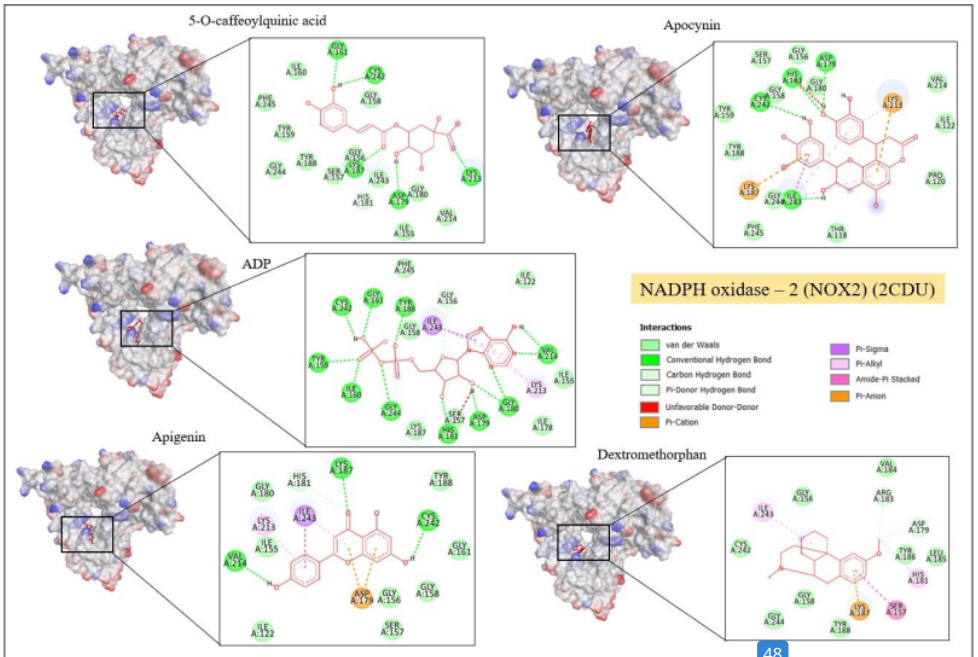

Figure 4. Interaction of ADP, 5-O-caffeoylquinic acid, apigenin, apocynin, and dextromethorphan with residues in the binding pocket of the 2CDU receptor.

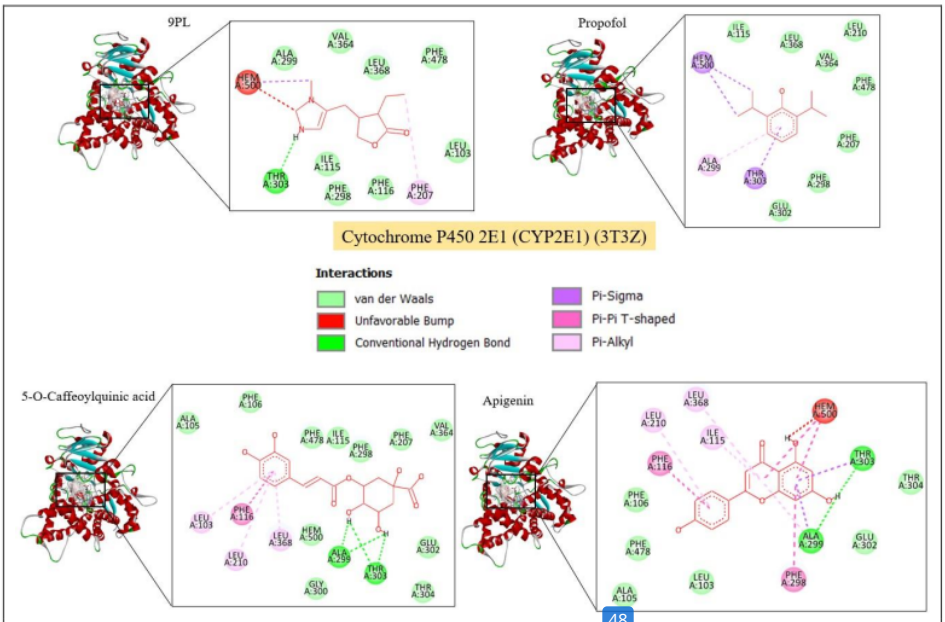

Figure 5. Interaction of 9PL, propofol, 5-O-caffeoylquinic acid, and apigenin with residues in the binding pocket of the 3T3Z receptor.

Ligand physicochemical based on Lipinski's rule

Predictions of the physicochemical properties of the ligands used in this research are presented in Table 3. The calculation of the physicochemical values determined were based on the Lipinski rule. The mono-CQAs (3-O-caffeoylquinic acid, 4-O-caffeoylquinic acid, and 5-O-caffeoylquinic acid) in *P. indica* leaves violated one rule, while the di-, tri-, and tetra caffeoylquinic acids violated three rules. Quercetin, kaempferol, luteolin, and apigenin have violation of the rules. Myricetin violated one rule. Quercetin 3-O-rhamnoside, quercetin 3-O-glucoside, quercetin 3-O-glucuronide, and kaempferol 3-O-β-D-glucopyranoside violated two rules.

ADME prediction

Table 4 describes the predicted absorption, distribution, metabolism, and excretion (ADME) properties of each ligand tested using the pkCSM online tool. Absorption studies can be carried out using various approaches. Generally, cell-based assays using cell lines such as Caco-2 and Madin-Darby canine kidney (MDCK) are performed for this purpose (Van de Waterbeemd et al., 2007). This study found that the Caco-2 permeability of apigenin has a value of >0.9, while the other test compounds have a value of <0.9. The intestinal absorption (human) of apigenin is >30% (93.25%). It shows that the apigenin compound has the potential to be well absorbed in the small intestine. Meanwhile, most CQAs and flavonoids in *P. indica* were predicted to have intestinal absorption values (human) >30%. The skin permeability value of the tested compounds was in the range of –2.735 (<2.5), which means that these compounds could penetrate the skin easily. All test compounds were predicted as P-glycoprotein substrates. All tested flavonoids were not inhibitors of P-glycoprotein I and II. 4,5-Di-O-caffeoylquinic acid methyl ester and 3,4,5-tri-O-caffeoylquinic acid methyl ester were predicted to be inhibitors of P-glycoprotein I. 3,4,5-Tri-O-caffeoylquinic acid methyl ester and 1,3,4,5-tetra-O-caffeoylquinic acid were P-glycoprotein II inhibitors.

The distribution parameters determined include VDss (human) (D_1), fraction unbound (human) (D_2), BBB permeability (D_3), and CNS permeability (D_4). The VDss value accepted was >–0.15. Thus, based on the prediction results, all tested compounds in this study met the criteria. Unfortunately, all tested compounds have BBB permeability values that did not meet the criteria (log BBB <0.3), which means that they have difficulty in penetrating the BBB. In this study, only kaempferol, luteolin, and apigenin were predicted to meet acceptable CNS permeability criteria because they have log P ≥–3. It means that these three compounds have the potential to penetrate the central nervous system.

Table 3. Physicochemical of ligands based on Lipinski's rule.

Compound Codes	MW (g/mol)	Log P	RB	HBA	HBD	TPSA	Number of violations
CA1	354.311	−0.6459	4	8	6*	141.587	1
CA2	354.311	−0.6459	4	8	6*	141.587	1
CA3	354.311	−0.6459	4	8	6*	141.587	1
CA4	516.455*	1.0296	7	11*	7*	209.119	3
CA5	516.455*	1.0296	7	11*	7*	209.119	3
CA6	516.455*	1.0296	7	11*	7*	209.119	3
CA7	530.482*	1.118	7	12*	6*	215.803	3
CA8	678.599*	2.7051	10	14*	8*	276.651	3
CA9	692.626*	2.7935	10	15*	7*	283.335	3
CA10	840.743*	4.3806	13	17*	9*	344.182	3
F1	302.238	1.988	1	7	5	122.108	0
F2	286.239	2.2824	1	6	4	117.313	0
F3	318.237	1.6936	1	8	6*	126.902	1
F4	286.239	2.2824	1	6	4	117.313	0
F5	270.24	2.5768	1	5	3	112.519	0
F6	448.38	0.4887	3	11*	7*	179.107	2
F7	464.379	−0.5389	4	12*	8*	183.901	2
F8	478.362	−0.4466	4	12*	8*	188.063	2
F9	448.38	−0.2445	4	11*	7*	179.107	2
RD1	583.498*	1.16812	8	11*	2	232.706	2
RD2	406.442	2.1273	4	5	1	172.995	0
RD3	271.404	3.3834	1	2	0	121.667	0
RD4	178.275	3.639	2	1	1	80.415	0
RD5	468.414	2.3983	2	10	7*	191.672	1

CA1: 3-O-Caffeoylquinic acid, CA2: 4-O-Caffeoylquinic acid, CA3: 5-O-Caffeoylquinic acid, CA4: 3,4-Di-O-Caffeoylquinic acid, CA5: 3,5-Di-O-Caffeoylquinic acid, CA6: 4,5-Di-O-Caffeoylquinic acid, CA7: 4,5-Di-O-Caffeoylquinic acid methyl ester, CA8: 3,4,5-Tri-O-Caffeoylquinic acid, CA9: 3,4,5-Tri-O-Caffeoylquinic acid methyl ester, CA10: 1,3,4,5-Tetra-O-Caffeoylquinic acid, F1: Quercetin, F2: Kaempferol, F3: Myricetin, F4: Luteolin, F5: Apigenin, F6: Quercetin 3-O-rhamnoside, F7: Quercetin 3-O-glucoside, F8: Quercetin 3-O-glucuronide, F9: Kaempferol 3-O-β-D-glucopyranoside, RD1: Fostemsavir, RD2: BMS-806, RD3: Dextromethorphan, RD4: Propofol, RD5: Apocynin, MW: molecular weight, RB: rotatable bonds, HBA: hydrogen bonds acceptor, HBD: hydrogen bonds donor, MR: Molar refractivity, TPSA: Topological polar surface area, Lipinski's rule of five: MW ≤500 g/mol, LogP ≤5, HBA (–N= or –O–) ≤10, HBD (–NH– or –OH) ≤5, (Turner and Agatonovic-Kustrin, 2007), *violation.

All tested compounds did not affect CYP2D6 and were not metabolized by it. The di-, tri-, and tetra-CQAs in this study were predicted to be able to act as CYP3A4 substrates. Quercetin, kaempferol, myricetin, luteolin and apigenin might act as CYP1A2 inhibitors. 3,4,5-Tri-O-Caffeoylquinic acid methyl ester could possibly act as CYP3A4 substrate and CYP3A4 inhibitor, while luteolin as CYP1A2 and CYP2C9 inhibitors. Apigenin was predicted as CYP1A2 and CYP2C19 inhibitors.

The excretion parameters determined were total clearance (E1) and renal OCT2 substrate (E2). The total clearance values of all flavonoids and mono-CQAs in this study were positive. It means they could be excreted quickly. On the other hand, the compounds di-, tri-, and tetra-CQAs have negative values. Furthermore, all compounds in this study were not substrates of the OCT2, which is involved in the uptake and secretion of cationic drugs.

Table 4. Prediction of ADME properties of ligands.

Compound Codes	A_1	A_2	A_3	A_4	A_5	A_6	A_7	D_1	D_2	D_3	D_4	M1	M2	M3	M4	M5	M6	M7	E_1	E_2
CA1	−2.449	−0.84	36.377	−2.735	Yes	No	No	0.581	0.658	−1.407	−3.856	No	No	No	No	No	No	No	0.307	No
CA2	−2.428	−0.892	20.029	−2.735	Yes	No	No	0.546	0.662	−1.593	−3.791	No	No	No	No	No	No	No	0.298	No
CA3	−2.449	0.84	36.377	−2.735	Yes	No	No	0.581	0.658	−1.407	−3.856	No	No	No	No	No	No	No	0.307	No
CA4	−2.955	−1.203	29.037	−2.735	Yes	No	No	1.633	0.294	−2.08	−3.804	No	Yes	No	No	No	No	No	−0.042	No
CA5	−2.952	−1.147	44.225	−2.735	Yes	No	No	1.7	0.28	−2.069	−3.822	No	Yes	No	No	No	No	No	−0.044	No
CA6	−2.955	−1.203	29.037	−2.735	Yes	No	No	1.633	0.294	−2.08	−3.804	No	Yes	No	No	No	No	No	−0.042	No
CA7	−2.981	−0.168	41.034	−2.735	Yes	Yes	No	1.902	0.234	−2.011	−3.798	No	Yes	No	No	No	No	No	−0.031	No
CA8	−2.899	−1.422	41.915	−2.735	Yes	No	No	1.521	0.166	−2.603	−3.768	No	Yes	No	No	No	No	No	−0.203	No
CA9	−2.894	−0.371	47.21	−2.735	Yes	Yes	Yes	1.604	0.194	−2.682	−3.811	No	Yes	No	No	No	No	Yes	−0.198	No
CA10	−2.892	−1.673	32.738	−2.735	Yes	No	Yes	0.572	0.269	−3.186	−3.765	No	Yes	No	No	No	No	No	−0.369	No
F1	−2.925	−0.299	77.207	−2.735	Yes	No	No	1.559	0.206	−1.098	−3.065	No	No	Yes	No	No	No	No	0.407	No
F2	−3.04	0.032	74.29	−2.735	Yes	No	No	1.274	0.178	−0.939	−2.228	No	No	Yes	No	No	No	No	0.477	No
F3	−2.915	0.095	65.93	−2.735	Yes	No	No	1.317	0.238	−1.493	−3.709	No	No	Yes	No	No	No	No	0.422	No
F4	−3.094	0.096	81.13	−2.735	Yes	No	No	1.153	0.168	−0.907	−2.251	No	No	Yes	No	Yes	No	No	0.495	No
F5	−3.329	1.007	93.25	−2.735	Yes	No	No	0.822	0.147	−0.734	−2.061	No	No	Yes	Yes	No	No	No	0.566	No
F6	−2.903	0.048	52.709	−2.735	Yes	No	No	1.517	0.13	−1.495	−4.156	No	No	No	No	No	No	No	0.364	No
F7	−2.925	0.242	47.999	−2.735	Yes	No	No	1.846	0.228	−1.688	−4.093	No	No	No	No	No	No	No	0.394	No
F8	−2.897	−1.061	25.112	−2.735	Yes	No	No	1.647	0.274	−1.614	−4.139	No	No	No	No	No	No	No	0.434	No
F9	−2.863	0.306	48.052	−2.735	Yes	No	No	1.444	0.218	−1.514	−3.908	No	No	No	No	No	No	No	0.462	No
RD1	−3.157	0.99	70.902	−2.735	Yes	Yes	No	−0.58	0.076	−2.035	−3.77	No	Yes	No	No	No	No	No	0.615	No
RD2	−3.229	1.898	71.86	−2.753	Yes	No	No	0.052	0.052	−1.148	−3.411	No	Yes	No	No	No	No	Yes	0.729	No
RD3	−4.13	1.657	97.234	−2.757	Yes	No	No	1.25	0.131	0.698	−1.11	No	Yes	No	No	No	Yes	No	0.964	Yes
RD4	-4.019	1.564	91.115	-1.77	No	No	No	0.703	0.093	0.497	-1.365	No	Yes	Yes	No	No	No	No	0.204	No
RD5	−2.901	−1.144	56	−2.735	Yes	Yes	Yes	0.379	0.125	−1.952	−3.738	No	No	No	No	No	No	No	0.039	No

CA1: 3-O-Caffeoylquinic acid, CA2: 4-O-Caffeoylquinic acid, CA3: 5-O-Caffeoylquinic acid, CA4: 3,4-Di-O-Caffeoylquinic acid, CA5: 3,5-Di-O-Caffeoylquinic acid, CA6: 4,5-Di-O-Caffeoylquinic acid, CA7: 4,5-Di-O-Caffeoylquinic acid methyl ester, CA8: 3,4,5-Tri-O-Caffeoylquinic acid, CA9: 3,4,5-Tri-O-Caffeoylquinic acid methyl ester, CA10: 1,3,4,5-Tetra-O-Caffeoylquinic acid, F1: Quercetin, F2: Kaempferol, F3: Myricetin, F4: Luteolin, F5: Apigenin, F6: Quercetin 3-O-rhamnoside, F7: Quercetin 3-O-glucoside, F8: Quercetin 3-O-glucuronide, F9: Kaempferol 3-O-β-D-glucopyranoside, RD1: Fostemsavir, RD2: BMS-806, RD3: Dextromethorphan, RD4: Propofol, RD5: Apocynin, ADME: absorption, distribution, metabolism, and excretion, A_1: Water solubility (log mol/L), A_2: Caco-2 permeability (log Papp in 10^{-6} cm.s^{-1}), A_3: Intestinal absorption (human) (% absorbed), A_4: Skin permeability (log Kp), A_5: P-glycoprotein substrate, A_6: P-glycoprotein I inhibitor, A_7: P-glycoprotein II inhibitor (A_{7+}), D_1: VDss (human) (log L/kg), D_2: Fraction unbound (human) (Fu), D_3: BBB permeability (log BB), D_4: CNS permeability (log P), M_1: CYP2D6 substrate, M_2: CYP3A4 substrate, M_3: CYP1A2 inhibitor, M_4: CYP2C19 inhibitor, M_5: CYP2C9 inhibitor, M_6: CYP2D6 inhibitor, M_7: CYP3A4 inhibitor, E_1: total clearance (log mL/min/kg), and E_2: renal OCT$_2$ substrate

Table 5. Prediction of toxicity properties of ligands.

Compound code	Predicted LD_{50} (mg/kg)	Predicted Toxicity Class	Hepatotoxicity	Carcinogenicity	Immunotoxicity	Mutagenicity	Cytotoxicity
CA1	5000	5	Inactive	Inactive	**Active**	Inactive	Inactive
CA2	5000	5	Inactive	Inactive	**Active**	Inactive	Inactive
CA3	5000	5	Inactive	Inactive	**Active**	Inactive	Inactive
CA4	5000	5	Inactive	Inactive	**Active**	Inactive	Inactive
CA5	5000	5	Inactive	Inactive	**Active**	Inactive	Inactive
CA6	5000	5	Inactive	Inactive	**Active**	Inactive	Inactive
CA7	1190	4	**Active**	Inactive	**Active**	Inactive	Inactive
CA8	5000	5	Inactive	Inactive	**Active**	Inactive	Inactive
CA9	5000	5	Inactive	Inactive	**Active**	Inactive	Inactive
CA10	5000	5	Inactive	Inactive	**Active**	**Active**	Inactive
F1	159	3	Inactive	**Active**	Inactive	**Active**	Inactive
F2	3919	5	Inactive	Inactive	Inactive	Inactive	Inactive
F3	159	3	Inactive	**Active**	Inactive	**Active**	Inactive
F4	3919	5	Inactive	**Active**	Inactive	**Active**	Inactive
F5	2500	5	Inactive	Inactive	Inactive	Inactive	Inactive
F6	5000	5	Inactive	**Active**	**Active**	Inactive	Inactive
F7	5000	5	Inactive	Inactive	**Active**	Inactive	Inactive
F8	5000	5	Inactive	**Active**	**Active**	Inactive	Inactive
F9	5000	5	Inactive	Inactive	Inactive	Inactive	Inactive
RD1	370	4	Inactive	Inactive	Inactive	Inactive	Inactive
RD2	1000	4	Inactive	Inactive	Inactive	Inactive	Inactive
RD3	116	3	Inactive	Inactive	Inactive	Inactive	Inactive
RD4	500	4	Inactive	Inactive	Inactive	Inactive	Inactive
RD5	2500	5	Inactive	Inactive	**Active**	Inactive	Inactive

CA1: 3-O-Caffeoylquinic acid, CA2: 4-O-Caffeoylquinic acid, CA3: 5-O-Caffeoylquinic acid, CA4: 3,4-Di-O-Caffeoylquinic acid, CA5: 3,5-Di-O-Caffeoylquinic acid, CA6: 4,5-Di-O-Caffeoylquinic acid, CA7: 4,5-Di-O-Caffeoylquinic acid methyl ester, CA8: 3,4,5-Tri-O-Caffeoylquinic acid, CA9: 3,4,5-Tri-O-Caffeoylquinic acid methyl ester, CA10: 1,3,4,5-Tetra-O-Caffeoylquinic acid, F1: Quercetin, F2: Kaempferol, F3: Myricetin, F4: Luteolin, F5: Apigenin, F6: Quercetin 3-O-rhamnoside, F7: Quercetin 3-O-glucoside, F8: Quercetin 3-O-glucuronide, F9: Kaempferol 3-O-β-D-glucopyranoside, RD1: Fostemsavir, RD2: BMS-806, RD3: Dextromethorphan, RD4: Propofol, RD5: Apocynin, LD_{50}: lethal dosage 50.

Toxicity prediction

CQAs are in class 5 based on their LD_{50} values, except 4,5-di-O-caffeoylquinic acid methyl ester, which is a compound in class 4 (See Table 5). Most of the flavonoids in this study are class 5; only quercetin and myricetin are class 3. Based on the GHS category, Class 1 includes compounds with LD_{50} ≤5 mg/kg, class 2 includes compounds with 5 < LD_{50} ≤ 50 mg/kg, class 3 includes compounds with 50 < LD_{50} ≤ 300 mg/kg, class 4 includes compounds with 300 < LD_{50} ≤ 2000 mg/kg), and class 5 includes compounds with LD_{50} >2000 mg/ (Gadaleta et al., 2019). All test compounds, except 4,5-di-O-caffeoylquinic acid methyl ester, have no potential for hepatotoxicity. All CQAs were not carcinogenic, while only kaempferol, apigenin, quercetin 3-O-glucoside, and kaempferol 3-O-β-D-glucopyranoside were not carcinogenic. All CQAs have the potential to have immunotoxicity properties, while from the flavonoid group in this study, quercetin, kaempferol, myricetin, luteolin, apigenin, and kaempferol 3-O-β-D-glucopyranoside did not have immunotoxicity properties. 1,3,4,5-tetra-O-caffeoylquinic acid, quercetin, myricetin, and luteolin were predicted to have mutagenicity. None of the test compounds have cytotoxicity properties.

DISCUSSION

Gp120 HIV-1 is a viral protein that plays an essential role in the initial life of the virus in human target host cells with the CD4 receptor. In summary, at-

tachment of gp120 to CD4 causes a conformational change of gp120, which subsequently allows the presentation of the chemokine co-receptor protein CXCR4 or CCR5 binding site together with gp41 (Caffrey, 2011; Sierra-Aragón and Walter, 2012). This process opens the way for HIV genetic material to enter host cell and initiate the HIV cycle itself. CYP2E1 and NADPH oxidase (NOX-2 and NOX-4) are activated due to the presence of viral particles, one of which is gp120, causing excess ROS production in cells (Ivanov et al., 2016). Excessive amounts of ROS can cause activation of nuclear factor (NF)-κB. This factor controls gene transcription, which can lead to increased HIV replication (Aquaro et al., 2008). Through molecular docking studies, predictions of the interaction of test compounds with specific receptor targets or proteins can help researchers search for and develop drug-candidate compounds (Najmi et al., 2022).

3TGS is a crystal structure of HIV-1 clade C strain C1086 gp120 core in complex with NBD-556 (Table S1). NBD-556 (native ligand 03G) is a small molecule (337.8 Da). This molecule binds to the Phe43 cavity of gp120 (Kwon et al., 2012) and shows its potential in targeting the inhibition of HIV-1 gp120 binding to host cells with the CD4 receptor (Tintori et al., 2013). In this study, it appears that the oxalamide NH in the native ligand 03G interacts with the Glu429, Met426, Gly473, and Asn425 amino acid residues with hydrogen bonds in the Phe43 cavity of 3TGS (Fig. 2) with a distance of 1.98, 2.14, 2.26, and 2.00 Å, respectively. According to Tintori et al. (2013), the oxalamide moiety of NBD-556 formed two hydrogen bonds with the carbonyl oxygen atoms of Asn425, Asp368, and Gly473 residues in the proposed Phe43 binding mode. In this study, the compounds 3,4-di-O-caffeoylquinic acid and quercetin 3-O-glucoside also interacted with Asn425 and Asp368 residues via hydrogen bonds. Previously, it was reported that the compound 3,4-di-O-caffeoylquinic acid interacts with HIV-1 integrase through molecular docking studies (Hu et al., 2010; Serina et al., 2016). This compound was assessed as having poor interaction with HIV-1 protease *in silico* (Serina et al., 2016).

Meanwhile, 3A1F and 2CDU are crystal structures of NOX. NOX is an enzyme that produces ROS (superoxide, $O_2^{\bullet-}$ or hydrogen peroxide, H_2O_2). The enzyme was identified in the membranes of phagocytic immune cells, namely macrophages and neutrophils (Vermot et al., 2021). NOX plays a role in pathogen killing by pumping ROS into the phagosome, where ingested pathogens can be destroyed. NOX also plays a role in cellular signaling, which is related to the processes of apoptosis, proliferation, homeostasis, and gene regulation (Couret and Chang, 2016). NOX is also commonly known as phagocytic NADPH oxidase (phox). There are several types of NOX, including NOX-1, NOX-2, NOX-3, NOX-4, NOX-5, dual oxidase-1 (DUOX-1) and DUOX-2. At the beginning of the entry of viral proteins into host cells, gp120 triggers the expression of NOX-2 and NOX-4. NOX-2 ($gp91^{phox}$) is an enzyme isolated from phagocytes with a molecular weight of 91 kDa. NOX-2 was the first NOX isoform identified. Meanwhile, NOX-4 is expressed most in the kidney, osteoclasts, fibroblasts, and endothelial cells. Its maturation depends on $p22^{phox}$. NOX-4 produces detectable H_2O_2 *in vitro* in the absence of superoxide dismutase (Vermot et al., 2021). By blocking NOX-2 and NOX-4, oxidative stress levels can be reduced (Reshi et al., 2014).

The 3A1F receptor does not have a native ligand, so docking is carried out using the blind docking method, where the binding set is determined according to studies by Vinay et al. (2020) by using VAS2870 as the target ligand. VAS2870 is an inhibitor of NOX isoforms (except NOX-3) (Vinay et al., 2020). Meanwhile, the native ligand used in the 2CDU receptor is ADP. Apocynin and dextromethorphan are used as reference inhibitors of NOX (Jiang et al., 2013; Da Silva Costa et al., 2018). In this study, compounds apocynin, 4-O-caffeoylquinic acid, and quercetin 3-O-glucuronide interacted with Gln123 and Ser91 residues in the 3A1F binding site via hydrogen bonds. Meanwhile, dextromethorphan only showed hydrogen bonds with Ser91. A study reported that phenolic derivative compounds anchored to the 3A1F receptor showed interactions with Ser91, Gln142, and Glu135 receptors via hydrogen bonds (Aqeel et al., 2020). Furthermore, in this study, the ligands ADP, 5-O-caffeoylquinic acid, apigenin, and apocynin both interacted with Cys242 and Asp179 residues in the 2CDU receptor binding site. Meanwhile, with Asp179 residue, dextromethorphan showed carbon-hydrogen bond interactions. According to Da Silva Costa et al. (2018), Asp179 is an amino acid residue that interacted via hydrogen bonds with the test ligand, namely two selected caffeine analogs, and via carbon-hydrogen bonds with dextromethorphan.

Cytochrome P450 (CYP) 2E1 (CYP2E1) is a family of heme-containing monooxygenase enzymes (Leung et al., 2013). In this study, the 3T3Z receptor, which is human CYP2E1 in complex with pilocarpine, was used. One study reported that the presence of gp120 showed the cause of increased expression of CYP2E1. They were involved in the production of ROS, which causes oxidative stress. Antioxidant activity associated with HIV-1 pathogenesis that acted on the CYP pathway could potentially be a new drug target (Reshi et al., 2014). There are several mechanisms of CYP2E1 inhibition, including haem ligation (4-methyl

pyrazole, 3-amino-1,2,4-triazole, and diallyl sulfide), haem interaction (disulphiram and phenethyl isothiocyanate), and competitive (propofol) (Lewis et al., 2000). In this study, 5-O-caffeoylquinic acid and apigenin were compounds that are good at interacting with 3T3Z (CYP2E1).

Failure of the drug its clinical application and unmanageable toxicity are closely related to the poor pharmacokinetics profile of the drug. Thus, initial evaluation by predicting ADMET properties using online tools is straightforward. It can reduce research costs compared to in vitro studies and shorten research time (Dulsat et al., 2023). In this study, predictions of the physicochemical and ADME properties of the test compounds were carried out using the pkCSM tool. The tool is considered to have an extensive range of ADME parameter information. Another advantage is that this tool can be accessed for free (Dulsat et al., 2023). Drug-likeness is related to the Lipinski rule of five (Turner and Agatonovic-Kustrin, 2007). This study found that the 3,4-di-O-caffeoylquinic acid is an anti-HIV candidate with a mechanism of action via attachment inhibition gp120-CD4. The compound also has antioxidant properties via NOX inhibition. However, the compound violated three Lipinski's rules. Based on the rule, if two or more criteria are violated, then the high-risk compound has oral bioavailability problems, such as poor absorption and permeation capabilities (Van de Waterbeemd et al., 2007). However, it should be noted that the rule does not definitely categorize whether a compound will be absorbed quantitatively well or poorly. In addition, compounds that do not violate the criteria are not always orally bioavailable. Thus, scientific proof regarding this matter is still needed. Even though the compound can be absorbed well, it can still have low bioavailability due to the presence of a high pre-systemic clearance system. In general, low bioavailability of marketed drugs may occur in oral dosage forms of hydrophobic chemical components and be absorbed slowly (Turner and Agatonovic-Kustrin, 2007).

As previously explained, the unmanageable toxicity of candidate compounds is also critical in their development as drugs. In this study, the ProTox-II webserver was used as a tool to predict the toxicity of tested compounds. The advantage of this tool is that it has extensive toxicity information, is easy to interpret, and is easily accessible for free (Banerjee et al., 2018). In this study, the toxicity of the compound 3,4-di-O-caffeoylquinic acid is predicted to be in class 5 as a compound that is categorized as safe. However, this compound is predicted to have potential immunotoxicity properties. Bhe et al. (2023) reported that the CQAs (especially 5-O-caffeoylquinic acid and 3,5-di-O-caffeoylquinic acid) found in coffee by-products have immunotoxin effects which could impact the immune system. However, the intake of both in coffee by-products is still considered relatively safe.

CONCLUSION

Based on this *in silico* study, CQAs and flavonoids from *P. indica* have the tential to act as anti-HIV and antioxidant agents. 3,4-Di-O-Caffeoylquinic acid was suggested to act as an anti-HIV by inhibiting gp120-CD4 attachment and as an antioxidant via NOX inhibition. The flavonoid that has the potential to be a good anti-HIV in this study was quercetin 3-O-glucoside. Antioxidant activity through NOX-2 inhibition was demonstrated by the 5-O-caffeoylquinic acid and apigenin, while NOX-4 inhibition was demonstrated by the 4-O-caffeoylquinic acid and quercetin 3-O-glucuronide. Meanwhile, 5-O-caffeoylquinic acid and apigenin were potential CYP2E1 inhibitors. By targeting the initial process of infection, drug candidates can be developed for HIV prevention and prophylaxis therapy. Based on ADMET predictions, there is a possibility that 3,4-di-O-caffeoylquinic acid compound experiences problems with oral bioavailability and immunotoxicity. However, in-depth studies, including experimental *in vitro* and *in vivo* studies, are required to validate the anti-HIV activity of the compounds further.

CONFLICT OF INTEREST

The authors declare no conflicts of interest.

ACKNOWLEDGMENTS

The authors thank the Directorate of Research and Development, Universitas Indonesia, for supporting this research [grant number: NKB-585/UN2.RST/HKP.05.00/2023].

REFERENCES

Alvin A, Miller KI, Neilan BA (2014) Exploring the potential of endophytes from medicinal plants as sources of antimycobacterial compounds. Microbiol Res 169:483–495. http://dx.doi.org/10.1016/j.micres.2013.12.009

Andarwulan N, Batari R, Sandrasari DA, Bolling B, Wijaya H (2010) Flavonoid content and antioxidant activity of vegetables from Indonesia. Food Chem 121: 1231–1235. https://doi.org/10.1016/j.foodchem.2010.01.033

Aqeel MT, Nisar-Ur-Rahman, Khan AU, Ahmad A, Ashraf Z, Rasheed U, Mansoor S (2020) Phenolic derivatives with antioxidant and anti-inflammatory activities: An *in silico*, *in vitro* and *in vivo* study. Pak Vet J 39: 598–602. https://doi.org/10.29261/pakvetj/2019.052

Aquaro S, Scopelliti F, Pollicita M, Perno CF (2008) Oxidative stress and HIV infection: Target pathways for novel therapies? Futur HIV Ther 2: 327–338. https://doi.org/10.2217/17469600.2.4.327

Arsiningtyas IS, Gunawan-Puteri MDPT, Kato E, Kawabata J (2014) Identification of α-glucosidase inhibitors from the leaves of *Pluchea indica* (L.) Less., a traditional Indonesian herb: promotion of natural product use. Nat Prod Res 28: 1350–1353. https://doi.org/10.1080/14786419.2014.904306

Banerjee P, Eckert AO, Schrey AK, Preissner R (2018) ProTox-II: A webserver for the prediction of toxicity of chemicals. Nucleic Acids Res 46: W257–W263. https://doi.org/10.1093/nar/gky318

Behne S, Franke H, Schwarz S, Lachenmeier DW (2023) Risk assessment of chlorogenic and isochlorogenic acids in coffee by-products. Molecules 28: 5540. https://doi.org/10.3390/molecules28145540

Bruxelle JF, Trattnig N, Mureithi MW, Landais E, Pantophlet R (2021) HIV-1 entry and prospects for protecting against infection. Microorganisms 9: 228. https://doi.org/10.3390/microorganisms9020228

Caffrey M (2011) HIV envelope: Challenges and opportunities for development of entry inhibitors. Trends Microbiol 19: 191–197. https://doi.org/10.1016/j.tim.2011.02.001

Chewchida S, Vongsak B (2019) Simultaneous HPTLC quantification of three caffeoylquinic acids in *Pluchea indica* leaves and their commercial products in Thailand. Rev Bras Farmacogn 29: 177–181. https://doi.org/10.1016/j.bjp.2018.12.007

Couret J, Chang TL (2016) Reactive oxygen species in HIV infection. EC Microbiol 3: 597–604. https://www.ncbi.nlm.nih.gov/pmc/articles/PMC5450819/

Da Silva Costa J, Da Silva Ramos R, Da Silva Lopes Costa K, Do Socorro Barros Brasil D, De Paula Da Silva CHT, Ferreira EFB, Dos Santos Borges R, Campos JM, Da Cruz Macêdo WJ, Dos Santos CBR (2018) An *in silico* study of the antioxidant ability for two caffeine analogs using molecular docking and quantum chemical methods. Molecules 23: 2801. https://doi.org/10.3390/molecules23112801

Dulsat J, López-Nieto B, Estrada-Tejedor R, Borrell JI (2023) Evaluation of Free online ADMET tools for academic or small biotech environments. Molecules 28: 776. https://doi.org/10.3390/molecules28020776

Ezzat S, Jeevanandam J, Egbuna C, Kumar S, Ifemeje J (2019) Phytochemicals as Sources of Drugs. In: Kumar S, Egbuna C (eds) Phytochemistry: An in-silico and in-vitro Update. Singapore: Springer Nature Singapore Pte Ltd, Gateway East, pp. 3–22. https://doi.org/10.1007/978-981-13-6920-9_1

Fan JR, Li H, Zhang HX, Zheng QC (2018) Exploring the structure characteristics and major channels of cytochrome P450 2A6, 2A13, and 2E1 with pilocarpine. Biopolymers 109: e23108. https://doi.org/10.1002/bip.23108

Forsythe SS, McGreevey W, Whiteside A, Shah M, Cohen J, Hecht R, Bollinger LA, Kinghorn A (2019) Twenty years of antiretroviral therapy for people living with HIV: Global costs, health achievements, economic benefits. Health Aff 38: 1163–1172. https://doi.org/10.1377/hlthaff.2018.05391

Gadaleta D, Vuković K, Toma C, Lavado GJ, Karmaus AL, Mansouri K, Kleinstreuer NC, Benfenati E, Roncaglioni A (2019) SAR and QSAR modeling of a large collection of LD50 rat acute oral toxicity data. J Cheminform 11: 58. https://doi.org/10.1186/s13321-019-0383-2

Heim KE, Tagliaferro AR, Bobilya DJ (2002) Flavonoid antioxidants: Chemistry, metabolism and structure-activity relationships. J Nutr Biochem 13: 572–584. https://doi.org/10.1016/S0955-2863(02)00208-5

Hikmawanti NPE, Saputri FC, Yanuar A, Jantan I, Ningrum RA, Mun'im A (2024) Insights into the anti-infective effects of *Pluchea indica* (L.) Less and its bioactive metabolites against various bacteria, fungi, viruses, and parasites. J Ethnopharmacol 320: 117387. https://doi.org/10.1016/j.jep.2023.117387

Hiryak K, Koren DE (2021) Fostemsavir: A novel attachment inhibitor for patients with multidrug-resistant HIV-1 infection. Ann Pharmacother 55: 792–797. https://doi.org/10.1177/1060028020962424

Hu Z, Chen D, Dong L, Southerland WM (2010) Prediction of the interaction of HIV-1 integrase and its dicaffeoylquinic acid inhibitor through molecular modeling approach. Ethn Dis 20: S1-45-9. https://www.ncbi.nlm.nih.gov/pmc/articles/PMC3089943/

Hussin M, Hamid AA, Abas F, Ramli NS, Jaafar AH, Roowi S, Majid NA, Dek MSP (2019) NMR-based metabolomics profiling for radical scavenging and anti-aging properties of selected herbs. Molecules 24: 3208. https://doi.org/10.3390/molecules24173208

Indrasetiawan P, Aoki-Utsubo C, Hanafi M, Hartati SRI, Wahyuni TS, Kameoka M, Yano Y, Hotta HAK, Hayashi Y (2019) Antiviral activity of *Cananga odorata* against hepatitis B virus. Kobe J Med Sci 65: E71–E79. https://www.ncbi.nlm.nih.gov/pmc/articles/PMC7012192

Ivanov A V., Valuev-Elliston VT, Ivanova ON, Kochetkov SN, Starodubova ES, Bartosch B, Isaguliants MG (2016) Oxidative stress during HIV infection: Mechanisms and consequences. Oxid Med Cell Longev 2016: 8910396. https://doi.org/10.1155/2016/8910396

Jiang J, Kang H, Song X, Huang S, Li S, Xu J (2013) A model of interaction between nicotinamide adenine dinucleotide phosphate (NADPH) oxidase and apocynin analogues by docking method. Int J Mol Sci 14: 807–817. https://doi.org/10.3390/ijms14010807

Kaur R, Sharma P, Gupta GK, Ntie-Kang F, Kumar D (2020) Structure-activity-relationship and mechanistic insights for anti-HIV natural products. Molecules 25: 2070. https://doi.org/10.3390/molecules25092070

Kongkiatpaiboon S, Chewchinda S, Vongsak B (2018) Optimization of extraction method and HPLC analysis of six caffeoylquinic acids in Pluchea indica leaves from different provenances in Thailand. Rev Bras Farmacogn 28: 145–150. https://doi.org/10.1016/j.bjp.2018.03.002

Kwon Y Do, Finzi A, Wu X, Dogo-Isonagie C, Lee LK, Moore LR, Schmidt SD, Stuckey J, Yang Y, Zhou T, Zhu J, Vicic DA, Debnath AK, Shapiro L, Bewley CA, Mascola JR, Sodroski JG, Kwong PD (2012) Unliganded HIV-1 gp120 core structures assume the CD4-bound conformation with regulation by quaternary interactions and variable loops. Proc Natl Acad Sci U S A 109: 5663–5668. https://doi.org/10.1073/pnas.1112391109

Lai Y-T (2021) Small molecule HIV-1 attachment inhibitors: Discovery, mode of action and structural basis of inhibition. Viruses 13: 843. https://doi.org/10.3390/v13050843

Leung T, Rajendran R, Singh S, Garva R, Krstic-Demonacos M, Demonacos C (2013) Cytochrome P450 2E1 (CYP2E1) regulates the response to oxidative stress and migration of breast cancer cells. Breast Cancer Res 15: R107. https://doi.org/10.1186/bcr3574

Lewis DFV, Bird MG, Dickins M, Lake BG, Eddershaw PJ, Tarbit MH, Goldfarb PS (2000) Molecular modelling of human CYP2E1 by homology with the CYP102 haemoprotein domain: Investigation of the interactions of substrates and inhibitors within the putative active site of the human CYP2E1 isoform. Xenobiotica 30: 1–25. https://doi.org/10.1080/004982500237794

Locher CP, Witvrouw M, De Bethune MP, Burch MT, Mower HF, Davis H, Lasure A, Pauwels R, De Clercq E, Vlietinck AJ (1996) Antiviral activity of Hawaiian medicinal plants against human immunodeficiency virus type-1 (HIV-1).

Phytomedicine 2: 259–264. https://doi.org/10.1016/S0944-7113(96)80052-3

Lu H, Tian Z, Cui Y, Liu Z, Ma X (2020) Chlorogenic acid: A comprehensive review of the dietary sources, processing effects, bioavailability, beneficial properties, mechanisms of action, and future directions. Compr Rev Food Sci Food Saf 19: 3130-3158. https://doi.org/10.1111/1541-4337.12620

Magaña AA, Kamimura N, Soumyanath A, Stevens JF, Maier CS (2021) Caffeoylquinic acids: chemistry, biosynthesis, occurrence, analytical challenges, and bioactivity. Plant J 107: 1299–1319. https://doi.org/10.1111/tpj.15390

Mahmood N, Moore PS, De Tommasi N, De Simone F, Colman S, Hay AJ, Pizza C (1993) Inhibition of HIV infection by caffeoylquinic acid derivates. Antivir Chem Chemother 4: 235–240. https://doi.org/10.1177/095632029300400406

Malik T, Chauhan G, Rath G, Murthy RSR, Goyal AK (2017) "Fusion and binding inhibition" key target for HIV-1 treatment and pre-exposure prophylaxis: Targets, drug delivery and nanotechnology approaches. Drug Deliv 24: 608–621. https://doi.org/10.1080/10717544.2016.1228717

Marković S, Tošović J (2016) Comparative study of the antioxidative activities of caffeoylquinic and caffeic acids. Food Chem 210: 585–592. https://doi.org/10.1016/j.foodchem.2016.05.019

McDougall B, King PJ, Wu BW, Hostomsky Z, Reinecke MG, Robinson WE (1998) Dicaffeoylquinic and dicaffeoyltartaric acids are selective inhibitors of Human Immunodeficiency Virus type 1 integrase. Antimicrob Agents Chemother 42: 140–146. https://doi.org/10.1128/aac.42.1.140

Mhya DH, Jakwa AG, Agbo J (2023) *In silico* analysis of antioxidant phytochemicals with potential NADPH oxidase inhibitory effect. J Heal Sci Med Res 41: e2022912. https://doi.org/10.31584/jhsmr.2022912

Mirani A, Kundaikar H, Velhal S, Patel V, Bandivdekar A, Degani M, Patravale V (2019) Tetrahydrocurcumin-loaded vaginal nanomicrobicide for prophylaxis of HIV/AIDS: *in silico* study, formulation development, and in vitro evaluation. Drug Deliv Transl Res 9: 828–847. https://doi.org/10.1007/s13346-019-00633-2

Najmi A, Javed SA, Al Bratty M, Alhazmi HA (2022) Modern approaches in the discovery and development of plant-based natural products and their analogues as potential therapeutic agents. Molecules 27: 349. https://doi.org/10.3390/molecules27020349

Phosrithong N, Samee W, Ungwitayatorn J (2012) 3D-QSAR studies of natural flavonoid compounds as reverse transcriptase inhibitors. Med Chem Res 21: 559–567. https://doi.org/10.1007/s00044-011-9570-z

Popović-Djordjević J, Quispe C, Giordo R, Kostić A, Katanić Stanković JS, Tsouh Fokou PV, Carbone K, Martorell M, Kumar M, Pintus G, Sharifi-Rad J, Docea AO, Calina D (2022) Natural products and synthetic analogues against HIV: A perspective to develop new potential anti-HIV drugs. Eur J Med Chem 233: 114217. https://doi.org/10.1016/j.ejmech.2022.114217

Quarta S, Scoditti E, Carluccio MA, Calabriso N, Santarpino G, Damiano F, Siculella L, Wabitsch M, Verri T, Favari C, Del Rio D, Mena P, De Caterina R, Massaro M (2021) Coffee bioactive n-methylpyridinium attenuates tumor necrosis factor (TNF)-α-mediated insulin resistance and inflammation in human adipocytes. Biomolecules 11: 1545. https://doi.org/10.3390/biom11101545

Reshi ML, Su YC, Hong JR (2014) RNA viruses: ROS-mediated cell death. Int J Cell Biol 2014: 467452. https://doi.org/10.1155/2014/467452

Rolnik A, Olas B (2021) The Plants of the Asteraceae Family as Agents in the Protection of Human Health. Int J Mol Sci 22: 3009. https://doi.org/10.3390/ijms22063009

Rudrapal M, Chetia D (2020) Virtual screening, molecular docking and QSAR studies in drug discovery and development programme. J Drug Deliv Ther 10: 225–233. http://dx.doi.org/10.22270/jddt.v10i4.4218

Salehi B, Anil Kumar NV., Şener B, Sharifi-Rad M, Kılıç M, Mahady GB, Vlaisavljevic S, Iriti M, Kobarfard F, Setzer WN, Ayatollahi SA, Ata A, Sharifi-Rad J (2018) Medicinal plants used in the treatment of human immunodeficiency virus. Int J Mol Sci 19: 1459. https://doi.org/10.3390/ijms19051459

Seitz R (2016) Human immunodeficiency virus (HIV). Transfus Med Hemotherapy 43: 203–222. https://doi.org/10.1159/000445852

Serina JC, Castilho PC, Fernandes MX (2016) Caffeoylquinic acids as inhibitors for HIV-I protease and HIV-I Integrase. A Molecular docking study. SDRP J Comput Chem Mol Model 1: 1–4.

Shaker B, Ahmad S, Lee J, Jung C, Na D (2021) *In silico* methods and tools for drug discovery. Comput Biol Med 137: 104851. https://doi.org/10.1016/j.compbiomed.2021.104851

Shin YH, Park CM, Yoon CH (2021) An overview of human immunodeficiency virus-1 antiretroviral drugs: General principles and current status. Infect Chemother 53: 29–45. https://doi.org/10.3947/IC.2020.0100

Sierra-Aragón S, Walter H (2012) Targets for inhibition of HIV replication: Entry, enzyme action, release and maturation. Intervirology 55: 84–97. https://doi.org/10.1159/000331995

Sreedevi A, Sangeetha S, Achari KMM, Sruthi KS, Vadlamudi Y (2022) Phytochemical, *in vitro* and *in silico* screening of roots of *Jasminum auriculatum* for antioxidant activity. Eurasian Chem Commun 4: 768–777. https://doi.org/10.22034/ecc.2022.330488.1331

Tamayose CI, dos Santos EA, Roque N, Costa-Lotufo L V, Pena Ferreira MJ (2019a) Caffeoylquinic acids: separation method, antiradical properties and cytotoxicity. Chem Biodivers 16: e1900093. https://doi.org/10.1002/cbdv.201900093

Tamayose CI, Torres PB, Roque N, Ferreira MJP (2019b) HIV-1 reverse transcriptase inhibitory activity of flavones and chlorogenic acid derivatives from *Moquiniastrum floribundum* (Asteraceae). South African J Bot 123: 142–146. https://doi.org/10.1016/j.sajb.2019.02.005

Tintori C, Selvaraj M, Badia R, Clotet B, Esté JA, Botta M (2013) Computational studies identifying entry inhibitor scaffolds targeting the Phe43 cavity of HIV-1 gp120. ChemMedChem 8: 475–483. https://doi.org/10.1002/cmdc.201200584

Turner JV, Agatonovic-Kustrin S (2007) *In silico* prediction of oral bioavailability. In: Taylor J, Triggle D (eds) Comprehensive Medicinal Chemistry II, 5: 699–724. https://doi.org/10.1016/B0-08-045044-X/00147-4

Van de Waterbeemd H, Testa B, Tillement J-P, Tremblay D, Laveé T, Funk C, Scherrmann J-M, Trager WF, Totah RA, Rettie AE, Oesch-Bartlomowicz B, Oesch F, Esser C, Parmentier Y, Bossant M-J, Bertrand M, Walther B, Artursson P, Neuhoff S, Matsson P, Tavelin S, Colombo P, Cagnani S, Sonvico F, Santi P, Russo P, Colombo G (2007) ADME-Tox Approaches. In: Taylor JB, Triggle DJ (eds) Comprehensive Medicinal Chemistry II, 5: 231–257. https://doi.org/10.1016/B0-08-045044-X/00125-5

Vermot A, Petit-Härtlein I, Smith SME, Fieschi F (2021) NAPDH oxidases (NOX): An overview from discovery, molecular mechanisms to physiology and pathology. Antioxidants 10: 890. https://doi.org/10.3390/antiox10060890

Vinay S, Yalamanchili K, Vinay S (2020) Assessing the efficacy of NOX enzyme inhibitors as potential treatments for ischemic

stroke *in silico*. J Emerg Investig 2: 1–7. https://doi.org/https://doi.org/10.59720/20-076

Vongsak B, Kongkiatpaiboon S, Jaisamut S, Konsap K (2018) Comparison of active constituents, antioxidant capacity, and α-glucosidase inhibition in *Pluchea indica* leaf extracts at different maturity stages. Food Biosci 25: 68–73. https://doi.org/10.1016/j.fbio.2018.08.006

Wardani AK, Mun'im A, Yanuar A (2018) Inhibition of HIV-1 reverse transcriptase of selected Indonesia medicinal plants and isolation of the inhibitor from *Erythrina variegata* L. Leaves. J Young Pharm 10: 169–172. https://doi.org/10.5530/jyp.2018.10.38

World Health Organisation (2023) HIV/AIDS-overview. https://www.who.int/health-topics/hiv-aids#tab=tab_1 [Consulted 16 Feb 2023].

AUTHOR CONTRIBUTION:

Contribution	Hikmawanti NPE	Saputri FC	Yanuar A	Jantan I	Yeni Y	Mun'im A
Concepts or ideas	x	x	x	x		x
Design	x	x	x	x		x
Definition of intellectual content	x	x	x			x
Literature search	x	x	x	x		x
Experimental studies	x				x	
Data acquisition	x				x	
Data analysis	x				x	
Statistical analysis	x				x	
Manuscript preparation	x				x	x
Manuscript editing	x					
Manuscript review	x	x	x	x	x	x

Citation Format: Hikmawanti NPE, Saputri FC, Yanuar A, Jantan I, Yeni Y, Mun'im A (2024) A computational approach to evaluate caffeoylquinic acids and flavonoids in *Pluchea indica* Less. leaves as potential anti-HIV agents. J Pharm Pharmacogn Res 12(4): 701–721. https://doi.org/10.56499/jppres23.1896_12.4.701

Supplementary data

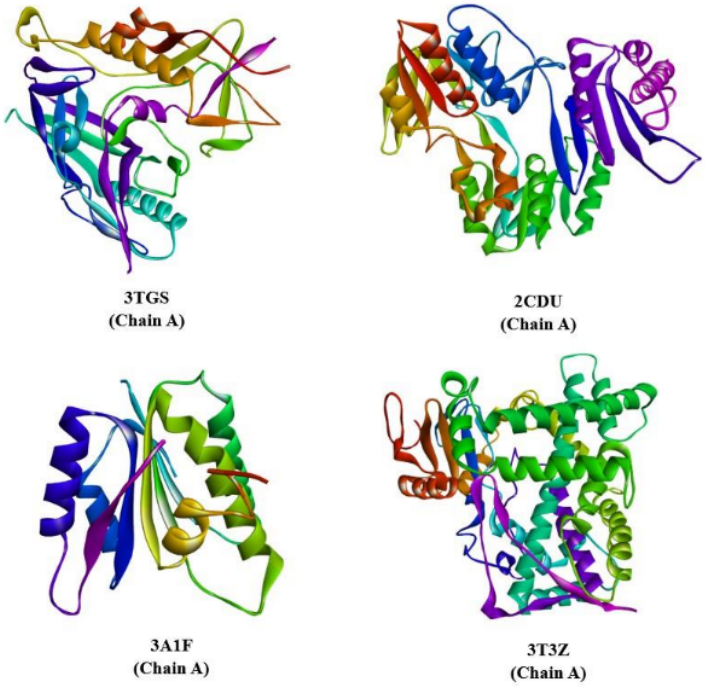

Figure S1. Structures of the receptors used in this study.

Tabel S1. Characteristics of the target receptors used in this study.

Targets	PDB ID*	Characteristics*	Ligands used in docking method validation	Reference drugs	Ref.
HIV-protein: Gp120	3TGS	• Crystal structure of HIV-1 clade C strain C1086 gp120 core in complex with NBD-556 • Organism: Human immunodeficiency virus 1 (HIV 1) • Expression System: *Homo sapiens* • Mutation: No • Method: X-ray diffraction • Resolution: 2.70 Å	N-(4-chlorophenyl)-N'-(2,2,6,6-tetramethylpiperidin-4-yl) ethanediamide (03G)*	Fostemsavir and BMS-806	(Kwon et al., 2012; Lai, 2021; Tintori et al., 2013)
Proteins related-oxidants: NADPH oxidase-4 ($gp91^{phox}$), NOX-4	3A1F	• The crystal structure of NADPH binding domain of gp91 (phox) • Organism: *Homo sapiens* • Expression System: *Escherichia coli* • Mutation: No • Method: X-ray diffraction • Resolution: 2.00 Å	VAS2870	Dextromethorphan and Apocynin	(Quarta et al., 2021; Sreedevi et al., 2022; Vinay et al., 2020)
NADPH oxidase-2 (NOX-2)	2CDU	• The Crystal Structure of Water-forming NAD(P)H Oxidase from *Lactobacillus sanfranciscensis* • Organism: *Fructilactobacillus sanfranciscensis* • Expression System: *Escherichia coli* • Mutation: No • Method: X-ray diffraction • Resolution: 1.80 Å	Adenosine-5'-diphosphate (ADP)*	Dextromethorphan and Apocynin	(Da Silva Costa et al., 2018; Mhya et al., 2023)
Cytochrome P4502E1 (CYP2E1)	3T3Z	• Human Cytochrome P450 2E1 in complex with pilocarpine • Organism: *Homo sapiens* • Expression System: *Escherichia coli* • Mutation: No • Method: X-ray diffraction • Resolution: 2.35 Å	(3S,4R)-3-ethyl-4-[(1-methyl-1H-imidazol-5-yl)methyl]dihydrofuran-2(3H)-one (9PL)*	Propofol	(Fan et al., 2018; Lewis et al., 2000)

*From RCSB Protein Data Bank (https://www.rcsb.org/).

ffeoylquinic_acids_and_flavonoids_in_Pluchea_indica_Less._...

ORIGINALITY REPORT

19%	16%	18%	11%
SIMILARITY INDEX	INTERNET SOURCES	PUBLICATIONS	STUDENT PAPERS

PRIMARY SOURCES

1	downloads.hindawi.com Internet Source	2%
2	Submitted to Universitas Airlangga Student Paper	1%
3	www.scribd.com Internet Source	1%
4	Submitted to University College London Student Paper	1%
5	Peyman Habibi, Henry Daniell, Carlos Ricardo Soccol, Maria Fatima Grossi-de-Sa. "The potential of plant systems to break the HIV-TB link", Plant Biotechnology Journal, 2019 Publication	1%
6	Submitted to Academic Library Consortium Student Paper	1%
7	Qi Qin, Fumi Tatsuzawa, Takahisa Nakane, Takashi Kaidzuka, Tsukasa Iwashina, Takayuki Mizuno. "Anthocyanins and Flavonols from the Flowers of *Ranunculus* Cultivars	1%

(Ranunculaceae) and Their Color Expression", The Horticulture Journal, 2024
Publication

8	www.journal.ugm.ac.id Internet Source	1 %
9	Ni Putu Ermi Hikmawanti, Fadlina Chany Saputri, Arry Yanuar, Ibrahim Jantan, Ratih Asmana Ningrum, Abdul Mun'im. "Insights into the anti-infective effects of Pluchea indica (L.) less and its bioactive metabolites against various bacteria, fungi, viruses, and parasites", Journal of Ethnopharmacology, 2023 Publication	1 %
10	Submitted to Birla Institute of Technology and Science Pilani Student Paper	1 %
11	www.hindawi.com Internet Source	<1 %
12	pubmed.ncbi.nlm.nih.gov Internet Source	<1 %
13	Igor Y. Iskusnykh, Evgenii D. Kryl'skii, Darya A. Brazhnikova, Tatyana N. Popova et al. "Novel Antioxidant, Deethylated Ethoxyquin, Protects against Carbon Tetrachloride Induced Hepatotoxicity in Rats by Inhibiting NLRP3	<1 %

Inflammasome Activation and Apoptosis", Antioxidants, 2021
Publication

14	mdpi-res.com Internet Source	<1 %
15	Submitted to Jacobs University, Bremen Student Paper	<1 %
16	www.researchgate.net Internet Source	<1 %
17	www.mdpi.com Internet Source	<1 %
18	Ernawati, Herman Suryadi, Abdul Mun'im. "Effect of gamma irradiation on the caffeoylquinic acid derivatives content, antioxidant activity, and microbial contamination of Pluchea indica leaves", Heliyon, 2021 Publication	<1 %
19	www.ncbi.nlm.nih.gov Internet Source	<1 %
20	Abel Kolawole Oyebamiji, Banjo Semire. "In-Silico Study on Anti-bacteria and Anti-fungal Activities of 3,4-Dihydropyrimidin-2(1H)-One Urea Derivatives", Chemistry Africa, 2020 Publication	<1 %
21	doaj.org Internet Source	

		<1 %
22	Matei, Marius Febi, Rakesh Jaiswal, and Nikolai Kuhnert. "Investigating the Chemical Changes of Chlorogenic Acids during Coffee Brewing: Conjugate Addition of Water to the Olefinic Moiety of Chlorogenic Acids and Their Quinides", Journal of Agricultural and Food Chemistry, 2012. Publication	<1 %
23	Connie Zhao, Hongru Li, Talia H. Swartz, Benjamin K. Chen. "The HIV Env Glycoprotein Conformational States on Cells and Viruses", mBio, 2022 Publication	<1 %
24	findresearcher.sdu.dk Internet Source	<1 %
25	coek.info Internet Source	<1 %
26	openaccess.izmirakademi.org Internet Source	<1 %
27	vital.seals.ac.za:8080 Internet Source	<1 %
28	Zhang, Hongmei, Mingxing Yin, Jinghua Shi, and Yanqing Wang. "Quest for the binding	<1 %

mode of malachite green with humic acid", Journal of Molecular Structure, 2015.
Publication

29	link.springer.com Internet Source	<1 %
30	Edible Medicinal And Non-Medicinal Plants, 2014. Publication	<1 %
31	Ibrahim Abuga, Shaida Fariza Sulaiman, Ridhwan Abdul Wahab, Kheng Leong Ooi, Mohammad Syaiful Bahari Abdull Rasad. "Phytochemical constituents and antibacterial activities of 45 Malay traditional medicinal plants", Journal of Herbal Medicine, 2021 Publication	<1 %
32	Submitted to Universitas Sultan Ageng Tirtayasa Student Paper	<1 %
33	cdn.repository.uisi.ac.id Internet Source	<1 %
34	nepis.epa.gov Internet Source	<1 %
35	"Drug Metabolism Prediction", Wiley, 2014 Publication	<1 %
36	Pandu Hariyono, Rini Dwiastuti, Muhammad Yusuf, Nurul H. Salin, Maywan Hariono. "2-	<1 %

	Phenoxyacetamide derivatives as SARS-CoV-2 main protease inhibitor: In silico studies", Results in Chemistry, 2022 Publication	
37	Submitted to Universitas Diponegoro Student Paper	<1 %
38	caps.ncbs.res.in Internet Source	<1 %
39	www.researchsquare.com Internet Source	<1 %
40	www.scielo.br Internet Source	<1 %
41	Hema Priya Manivannan, Vishnu Priya Veeraraghavan, Arul Prakash Francis. "Identification of molecular targets of Trigonelline for treating breast cancer through network pharmacology and bioinformatics-based prediction", Molecular Diversity, 2023 Publication	<1 %
42	Zizovic, I.. "Supercritical carbon dioxide extraction of sesquiterpenes from valerian root", The Journal of Supercritical Fluids, 200712 Publication	<1 %
43	www.science.gov Internet Source	<1 %

44	Daniel Augustynowicz, Klaus Peter Latté, Michał Tomczyk. "Recent phytochemical and pharmacological advances in the genus Potentilla L. sensu lato – An update covering the period from 2009 to 2020", Journal of Ethnopharmacology, 2021 Publication	<1 %
45	m.moam.info Internet Source	<1 %
46	ujcontent.uj.ac.za Internet Source	<1 %
47	Remya Ramachandran Surajambika, Pavithra Palanikarasu. " 2D-QSAR Modeling, Docking, Synthesis and Evaluation of Novel Flavone Derivatives as Anticancer Agents ", Current Bioactive Compounds, 2024 Publication	<1 %
48	Viktor Hornak, Robert Abel, Asim Okur, Bentley Strockbine, Adrian Roitberg, Carlos Simmerling. "Comparison of multiple Amber force fields and development of improved protein backbone parameters", Proteins: Structure, Function, and Bioinformatics, 2006 Publication	<1 %
49	tel.archives-ouvertes.fr Internet Source	<1 %

50	"Evidence Based Validation of Traditional Medicines", Springer Science and Business Media LLC, 2021 Publication	<1 %
51	Nizar Mohammad Abuharfeil, Mahmoud Mohammad Yaseen, Fawzi M. Alsheyab. "Harnessing Antibody-Dependent Cellular Cytotoxicity To Control HIV-1 Infection", ACS Infectious Diseases, 2018 Publication	<1 %
52	Rocha, Jamira Dias. "Avaliação dos Efeitos Biológicos e Tóxicos de Plantas do Cerrado : Um Enfoque em Vernonanthura Polyanthes", Universidade Estadual de Goiás (Brazil), 2024 Publication	<1 %
53	ir.cut.ac.za Internet Source	<1 %
54	krishikosh.egranth.ac.in Internet Source	<1 %
55	papyrus.bib.umontreal.ca Internet Source	<1 %
56	www.hilarispublisher.com Internet Source	<1 %
57	www.karger.com Internet Source	<1 %

Exclude quotes	Off	Exclude matches	Off
Exclude bibliography	On		